DOT/FAA/CT-94/80

FAA Technical Center
Atlantic City International Airport,
N.J. 08405

HINCOF-I: A Code for Hail Ingestion in Engine Inlets

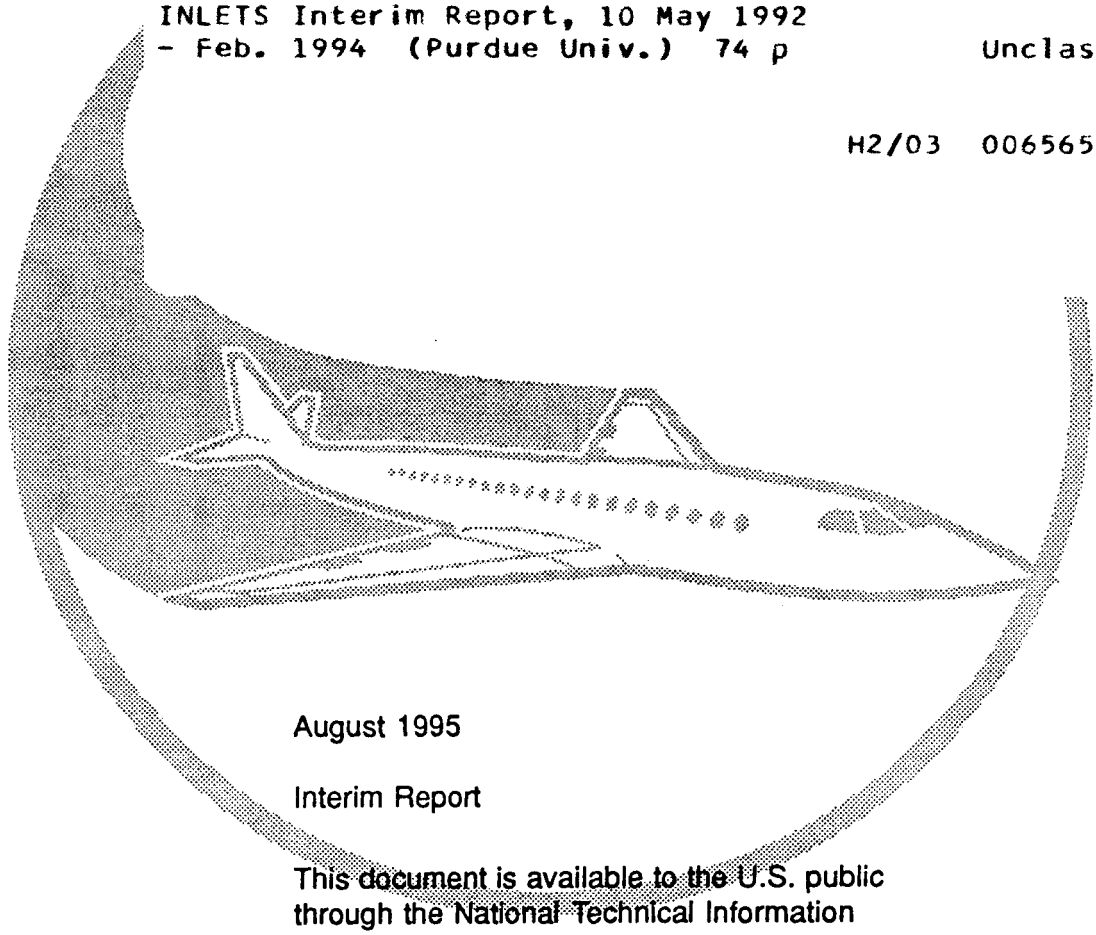

August 1995

Interim Report

U.S. Department of Transportation
Federal Aviation Administration

NOTICE

This document is disseminated under the sponsorship of the U. S. Department of Transportation in the interest of information exchange. The United States Government assumes no liability for the contents or use thereof.

The United States Government does not endorse products or manufacturers. Trade or manufacturers' names appear herein solely because they are considered essential to the objective of this report.

ACKNOWLEDGMENTS

The research work is supported by the Federal Aviation Administration (FAA) under Grant No. 92-G-002. Mr. J. Wilson is the FAA technical monitor, and his valuable encouragement is appreciated.

TABLE OF CONTENTS

		Page
EXECUTIVE SUMMARY		ix
1.	INTRODUCTION	1
	1.1 Background	1
	1.2 Hail Properties	1
	1.3 Hail Appearance in the Engine Capture Streamtube	2
	1.4 Processes Associated with Hail Motion	3
	1.5 Inlet and Spinner Geometry	3
	1.6 Outline of Report	4
2.	DESCRIPTION OF HINCOF-I CODE	4
	2.1 Air Flowfield Through an Inlet	4
	2.2 Motion of Hailstones	5
	2.2.1 Describing Equations for Hail Motion	5
	2.2.2 Impact, Surface Motion, and Rebound	5
	2.2.3 Melting and Sublimation	8
	2.2.4 Hail Adhesion	9
	2.2.5 Break-Up	9
	2.3 Model for the Appearance of Hailstones in the Air Capture Streamtube	11
	2.4 Ingestion Parameters	11
	2.5 Numerical Procedure	12
	2.6 List of Variables	13
	2.7 Description of Subroutines	13
3.	INPUT AND OUTPUT	14
	3.1 Input	14
	3.2 Output	15
4.	ILLUSTRATIVE CASE	16
	4.1 The Basic Illustrative Case	17
	4.1.1 Input	18
	4.1.2 Output	18
	4.1.3 Results	29

4.2 The Other Test Cases 30
4.2.1 Effect of Shape of Spinner 30
4.2.2 Effect of Inlet Flow Conditions 30
4.2.3 Effect of Hail Ingestion Conditions 31

5. DISCUSSION 32

6. REFERENCES 34

APPENDICES

A Methodology for Determining Air Flowfield of Engine Inlets
B Listing of Variables
C Listing of Subroutines

LIST OF FIGURES

Figure		Page
1	Sketch of Inlet with Different Spinners	35
2	Probability Density Functions	36
3	Flowchart of the Numerical Scheme	37

LIST OF TABLES

Table		Page
1	Mechanical Properties of Common Inlet Materials	2
2	Thermal Properties of Hail and Ice	2
3	Estimates of Hail Ingestion	2
4	Effect of Incident Normal Velocity and Contact Area on Impact Stress	11
5	Hail Properties for Illustrative Cases	16
6	Illustration Cases	17
7	Ingestion Results for All Groups	29

EXECUTIVE SUMMARY

Hail ingestion into engines is one of the recognized hazards during aircraft flight through hail storms. The hail stones entering the engine inlet can be expected to affect all parts of the engine along the flowpath of the working fluid, while the hailstones undergo various types of change in size, shape, and structure, including phase transformation. The consequences may involve setting in of vibration and mechanical damage to engine parts, and also, changes in engine performance such as power loss, surging of the compression system, and occasionally flameout. It is thus of considerable importance to be able to determine the occurrence of such effects in relation to atmospheric and flight conditions in advancing engine design and operational procedures, including engine testing on-ground for ability to meet desired safety requirements.

As part of a multi-faceted program of research on hail ingestion and its effects, the current report deals with an investigation on the basic problem of determining the time rate of ingestion of hailstones — the total quantity and distribution — at the engine face for given inlet geometry, engine operation, and hail-laden atmospheric conditions. The distribution is particularly significant as it is of considerable interest in the case of a bypass turbofan engine to determine the fraction entering the core stream in relation to that escaping into the bypass stream.

Considering the capture streamtube in front of an inlet supplying air to an operating engine during a hail storm, one can expect inhomogeneities in several aspects of hailstones: size, spatial and temporal distribution, velocity, and physical characteristics. At a cross-sectional plane selected in the capture streamtube, sufficiently far ahead of the inlet entry plane, the hail properties and motion may, therefore, be identified only in terms of random values — albeit within certain ranges of variables — or probability functions at a given instant of time during ingestion. Thus, at a later time during ingestion, there appears another set of randomly identified values for each of the characteristics of hailstones.

The physical properties of hailstones are not well established, especially considering their state at flight attitudes, during or immediately following their formation and growth. During motion of hailstones, considering friction, heat and mass transfer, impact, rolling and rebound, and shattering into fragments, it is essential to have a knowledge of the structure of hailstones including occlusions, if any, the density, the hardness, the modulus of electricity, the coefficients of restitution, and the heat conductivity and sublimation characteristics. Unfortunately, there are little unambiguous data that can be utilized under flight or even simulated ground conditions for hailstones. During on-ground testing, it is invariably the practice to utilize ice in some compacted form as a substitute for hail. However, ice, whose characteristics are different from those of hail, is a substance that appears in many states with different properties. Currently characterization of hail may only be done in part on data on hailstones and in many respects on those for ice. However, some processes, especially rebound, phase change, and shattering, are highly sensitive to the physical properties. For example, a hailstone on impact may experience rolling over the surface depending upon the coefficients of restitution and wetting, and this may affect the direction, if not the possibility, of rebound for a given angle of impact. The interactive processes between the hailstone and the impacted body depend upon the properties of both materials and their surfaces.

The prediction of hail motion through an inlet and ingestion at the engine face has been set up by developing a numerical scheme, designated HINCOF-I. The code is divided into two parts: one for the prediction of air flow, which is assumed to be independent of the presence of (the small volume of) hail, and a second for the prediction of hail motion. In the latter, provision has been made to include the friction drag, impact of hail with one another and boundary walls, heat and mass transfer during motion and impact, and shattering.

The numerical procedure incorporated in the code is the Monte-Carlo procedure. Using that scheme it is possible to include probability distributions for the size of the hailstones, their appearance in space and time at a suitable location in the capture streamtube, and their velocity. The convergence criterion utilized is that the change in ingestion at the engine face must not exceed a specified value in successive simulations.

The current report includes a detailed description of the HINCOF-I code and several illustrative cases. The code includes inlet geometry, and air flow, hail, and engine operation characteristics in parametric form so that any desired set of conditions can be included in a specific calculation.

One of the chief design innovations for diverting the hailstones into the bypass stream in a turbofan engine is to utilize an elliptic shape for the spinner as it is expected that the rebound of hailstones depends upon the curvature of the spinner, among various characteristics, for given impact direction and velocity. This is confirmed, in general, by the predictions obtained by using the HINCOF-I code for elliptic and conical spinners with identical ingestion conditions. However, it is found that when the hailstones are substantially present in small sizes, an elliptic spinner is not more effective than a conical spinner.

The various test case conditions investigated may be grouped under (i) effect of inlet flow conditions including velocity of air flow, size of the inlet, and cross-flow into the inlet due to operation at an angle of attack, (ii) effect of hail ingestion conditions including size of hailstones and size distribution of hailstones, and (iii) effect of hail properties. The parameter that has a dominant influence in all cases is the size and size distribution of hailstones, smaller sizes leading to increased ingestion at the engine face. Ingestion is in general lower at the engine face when the velocity of air flow is increased, and the size of the inlet is small. A cross-flow into the inlet gives rise to a reduction in ingestion and a substantial asymmetry across the plane of the angle of attack. The hail properties such as elasticity, coefficients of restitution, and conductivity and sublimation affect the hailrolling, melting, sticking, pealing, rebounding, and shattering under different circumstances and, therefore, have a major influence on hail ingestion and, especially, distribution at the engine face. The code can be used to determine, if only to determine the trends qualitatively, the influence of such properties; however, a detailed experimental study on a specially built cascade tunnel with well-characterized ice particles is required before further advances can be made in predictions in relation to the influence of hail characteristics.

1. INTRODUCTION.

During flight operations under various types of inclement weather conditions, hail ingestion into turbine engines is a major concern. A number of adverse effects are known to occur sometimes in a turbine engine when ingesting hail: for example, power loss, surging, and occasionally flameout. There is, considerable uncertainty and controversy in the precise relations between the hail characteristics and the ingestion and also the observed or perceived effects on the engine. Engine testing on the ground may generally be conducted only with simulated hailstones, for example compacted ice balls, and under air flow and injection conditions that may reproduce actual ingestion conditions in some, but not all, conditions. An attempt at developing a prediction scheme for hail ingestion and its effects on engine performance also becomes only partially successful in view of the lack of comprehensive and reliable data on the aero-thermo-mechanical properties of hail stones. It is generally agreed that an approach for establishing the hail ingestion effects may be hybrid in nature, a combination of testing, and analysis and prediction. This report deals with a numerical method for establishing hail ingestion through an engine inlet to the engine face for given atmospheric conditions and engine operating setting. The prediction code has been named HINCOF-I.

1.1 BACKGROUND.

Establishing hail ingestion into an engine from the atmosphere requires some principal considerations as follows:

(i) hail properties,
(ii) hail appearance in the engine air capture tube,
(iii) processes associated with hail motion, and
(iv) inlet geometry, including that of the spinner.

A detailed discussion on items (i), (ii), and (iii) is provided in reference 1. Here, a brief account is presented regarding those items and also item (iv), considering those aspects that are directly related to the set up and use of the HINCOF-I code.

1.2 HAIL PROPERTIES.

The mechanical properties of interest are listed in table 1. Little data exist for hail stones in the formation and growth stages in the upper atmosphere. Parametric studies are based on data obtained in ground test facilities for hail and also for ice compacted in various ways. Such data do not include information on the inhomogeneity of the "model" hailstones in relation to the inhomogeneity observed in selected cases in the atmosphere. However, based on available data one can select ranges of values for various properties, and an example of ranges is presented in table 1. Table 1 also contains some properties for materials generally utilized in the construction of engine inlets and spinners. These are of interest in relation to impact related processes occurring during hailstone ingestion.

TABLE 1. MECHANICAL PROPERTIES OF COMMON INLET MATERIALS

Property	Hail/Ice	Al-Alloy
Compressive strength, MPa.	2.5-12.5	345
Youngs' Modulus, GPa.	9.09-11.10	70-80
Coeff. of kinetic friction	0.02-0.09	-

Table 2 provides the range of values for the density of hail and the density of ice. The thermal properties are provided in table 2 only for ice since they are not known for hail. In performing calculations the thermal properties for hail are assumed to be the same as for ice.

TABLE 2. THERMAL PROPERTIES OF HAIL AND ICE

Property	Hail	Ice
Density, kg/m^3	850-917	920
Latent heat of sublimation, J/kg	-	2558.2
Latent heat of fusion/melting, J/kg	-	333.35
Specific Heat Capacity, J/kg/K	-	210.6
Thermal Conductivity, W/m/K	-	2.22

1.3 HAIL APPEARANCE IN THE ENGINE CAPTURE STREAMTUBE.

The growth of hail stones, starting from an embryo stage, depends upon the updrafts that arise in the atmosphere. The number density (that is, number per unit volume of atmosphere) and the size distribution of hail stones may vary appreciably in the atmosphere and in the engine air capture streamtube. Table 3 presents an estimate of the total volume of hail that can be expected to enter the air capture streamtube for an inlet of a typical bypass turbofan engine with an area of cross-section at the highlight of about 3.5-4.0 sq.m. under different conditions, noting that the fraction of water content may be about 10 per cent by mass of air flow or volumetrically about 10 cc per unit cubic meter of air.

TABLE 3. ESTIMATES OF HAIL INGESTION

	Case A	Case B	Case C	Case D
Altitude, m	3,000	Sea Level	3000	10,000
Density of air, kg/m^3	0.9053	1.2256	0.9053	0.41351
Mach number of flight	0.3	0.3	0.5	0.8
Volume of hail ingested, cc/s	400 - 700	400 - 700	1000 - 1400	1000 - 1400

An engine inlet and its capture streamtube may be considered, in general, to be axisymmetric, although one may occasionally find a three-dimensional frontal cross-section for an inlet. In the axisymmetric case, considering a radial plane in front of the engine, the appearance of hail stones can be described in terms of the combination of all of the following parameters:

i. characteristic size,
ii. location of appearance,
iii. frequency of appearance, and,
iv. velocity.

Referring to figure 1, a radial plane is shown in the capture tube in front of a typical subsonic inlet. It is clear that each of the four parameters mentioned above can vary, in practice, randomly over the radial plane. Thus different size hailstones may appear at random locations, in random intervals of time, and with random velocity over the radial plane at a streamtube location in the capture tube far upstream in the atmosphere.

1.4 PROCESSES ASSOCIATED WITH HAIL MOTION.

During the motion of hail, along with air, in the capture tube and the inlet, the hailstone is subjected to aerodynamic frictional drag, gravitational action, heat and mass transfer, collisions with other hailstones, and impact, rebound and break-up into smaller entities. Impact here denotes collision with a surface of the inlet. It is necessary to account for each of the hailstones in establishing the trajectory and the possibility of ultimately arriving at the engine face.

In general it is difficult to separate the processes of heat and mass transfer, collisions with other hailstones, and impact, rebound, and break-up. Heat and mass transfer can arise entirely due to frictional heating and the difference between the temperatures of a hailstone and the atmosphere. They can also arise during collisions and impact.

The impact and rebound processes have various complexities: (i) In view of the existence of kinetic friction between a hailstone and a surface of an inlet, rebound is governed by both the tangential and the normal coefficients of restitution. (ii) In addition to sliding there may also be rolling motion following impact. And, (iii) a hailstone is subjected to break-up and shattering based on the relation between the impact stress and the compressive strength of the hailstone. Each of the preceding involves considerable controversy in view of the effects of inhomogeneity in the structure of a hailstone.

One approach to including these processes in establishing the motion of hailstones is to treat each of the processes both individually and also interactively whenever necessary and feasible.

1.5 INLET AND SPINNER GEOMETRY.

The inlet geometry has an influence on the capture streamtube area and the scoop factor. The physical size of the inlet also governs those parameters. The spinner is usually either conical or super-elliptical. The shape and size of the spinner determine principally the impact and rebound processes. They can, therefore, be optimized to control the number and size of hailstones entering at the engine face.

1.6 OUTLINE OF REPORT.

This report presents a description of the HINCOF-I code which has been set up to determine the motion and eventual ingestion at the engine face of hailstones from the atmosphere through the engine inlet. A description of the code is given in the next section. The input for using the code and the output are presented in the following section. Finally, a test case is given for illustrating the use of the code. In determining the motion of hailstones it is assumed that the motion of air can be established independently and separately. Two methods for determining the air flowfield are described in appendix A of this report.

2. DESCRIPTION OF HINCOF-I CODE.

The HINCOF-I code provides a numerical procedure for establishing the ingestion of hailstones from the atmosphere through an engine inlet at the engine face, for given atmospheric, flight, and engine operating conditions. The engine inlet is taken to include the spinner. The engine face is assumed to coincide with a fan entry section in a fan-engine, and the compressor entry section when a compressor is present immediately following the inlet.

The atmospheric conditions consist of air properties, air flow properties if the atmosphere includes any motions, and details about the hail present. It is possible that the atmosphere has a content of water in other forms such as water vapor and liquid water. Water vapor can be included in the description of air composition. The presence of liquid water cannot be handled with the HINCOF-I code.

The flight operating conditions of interest are the flight speed and cross-flow, if any. It is well known that in regions of hail formation and growth at altitude, strong updrafts are usually present, and they give rise to an angle of attack for the inlet relative to the air stream.

The engine operating conditions refer to the mass flow demanded by the engine, and hence, to a capture streamtube in front of the inlet, a velocity and a mass flow at entry into the inlet, and a spillage of air to the outside from the capture streamtube.

In the HINCOF-I code, the air flowfield is determined taking into account the atmosphere, flight operation, and engine operation conditions. However, the presence of hailstones is not accounted for in determining the air flowfield since the total volume of hailstones ingested per unit time is quite small relative to the total volume of airflow per unit time.

2.1 AIR FLOWFIELD THROUGH AN INLET.

Several procedures are available for determining the flowfield of air through an engine inlet, including the capture streamtube and accounting for the presence of a spinner. Two of the procedures are described in appendix A of this report.

2.2 MOTION OF HAILSTONES.

The motion of hailstones in the air capture streamtube and the inlet (figure 1) is determined in an air flowfield that is established, as stated earlier, independently of the presence of hailstones. The hailstones are assumed to be subject to the following processes.

2.2.1 Describing Equations for Hail Motion.

The Lagrangian equations of motion for hailstone of mass m_h in the (x,y,z) coordinates in a given (y,z) plane are as follows:

$$\ddot{x} = \frac{k}{m_h}(U_a - \dot{x})\sqrt{(U_a - \dot{x})^2 + (V_a - \dot{y})^2} \tag{1}$$

$$\ddot{y} = \frac{k}{m_h}(V_a - \dot{y})\sqrt{(U_a - \dot{x})^2 + (V_a - \dot{y})^2} - g \tag{2}$$

where $k = \frac{1}{2}\rho_a C_D A_p$, and A_p is the cross-sectional area of the hailstone. The following relation is used for C_D the draft coefficient (reference 1):

$$C_D = \begin{cases} \frac{24}{Re}\left(1 + \frac{Re^{0.66}}{6.0}\right) & Re < 1000 \\ 0.44 & otherwise \end{cases} \tag{3}$$

where Re is the particle Reynolds number. U_a and V_a represent the components of air velocity in the x and y directions, respectively, ς_a, the density of air, and y, the acceleration due to gravity.

2.2.2 Impact, Surface Motion, and Rebound.

The impact and rebound process for a hailstone striking a solid surface depends upon the following (reference 2): (i) relative normal velocity, (ii) radius of curvature of the impacting bodies, (iii) the Youngs' moduli and Poisson's ratio of the material of the bodies, (iv) the coefficient of friction static and kinetic), and (v) the normal coefficient of restitution. Here, the static friction force is the force required to move a body from rest, and the kinetic friction force is the force required to sustain sliding motion.

The rebound velocity of a hailstone can be determined from the values of the reduced moduli for the impacting bodies, the contact force, and the contact time. The impact process is considered as a superposition of tangential and normal impact, the latter referred to as the Hertz impact. The reduced modulus of the impacting bodies is given by the following expression:

$$E_r = \left(\frac{1 - V_1^2}{\pi E_1} + \frac{1 - V_2^2}{\pi E_2} \right)^{-1} \tag{4}$$

where body 1, for example, may represent the inlet or the spinner, and body 2 denotes the hailstone. In order to determine the contact time and force, it is necessary to determine a so-called distance of approach between the colliding bodies. The distance of approach, α, may be expressed as follows:

$$= \alpha_o \sin(\pi t / t^*) \tag{5}$$

where α_o denotes the maximum value of α, given by:

$$_o = \left[1.25 \left(V_{1n} - V_{2n} \right)^2 / n n_1 \right]^{0.4} \tag{6}$$

and n and n_1 are given by:

$$n = \sqrt{8 / \beta} E_r / 3\pi \tag{7}$$

$$n_1 = \frac{m_1 + m_2}{m_1 m_2} \tag{8}$$

Here, β represents the average curvature of the impacting bodies, and is given by:

$$\beta = \frac{1}{2} \left(\frac{1}{R_1} + \frac{1}{R_2} \right) \tag{9}$$

The time of contact, t*, and the contact force, P, can then be expressed in terms of α as follows:

$$t^* = 2.943 \alpha_o / \left(V_{1n} - V_{2n} \right) \tag{10}$$

$$P = P_o \sin\left(\pi t / t^* \right) \mathrm{P} \tag{11}$$

where

$$P_o = n \alpha_o^{3/2} \tag{12}$$

the area of contact, A, is given by

$$A = A_o \sin\left(\pi t / t^* \right) \tag{13}$$

where A_o is the maximum area of contact, given by:

$$A_o = \pi \frac{\alpha_o}{2\beta} \tag{14}$$

The final tangential velocity of the hailstone at the end of the period of contact is obtained by accounting for the action of the frictional force as follows: The frictional force which resists motion in the tangential direction is given by:

$$F_k = \mu_k P \tag{15}$$

The change in the tangential velocity after impact then is given by:

$$\left(V_{1tf} - V_{2tf}\right) = \int_0^{t_{slip}} \frac{F_k}{m_1} dt + \left(V_{1to} - V_{2to}\right) \tag{16}$$

where the subscripts, o and f, denote the initial and the final velocities, respectively, and t_{slip} denotes the time of slipping or sliding motion. The latter period of time may be different from the time of contact t*. The time of slip t_{slip} can be determined as follows: When a body slides relative to another surface, the frictional force imparts angular momentum to that body. When the angular velocity attained by the body due to this angular momentum is such that the relative tangential velocity at the contact point becomes zero, the body stops sliding and transitions to a pure rolling mode, giving rise to a reversal in the direction of friction and a change in the magnitude of the frictional force from F_k to F_s. The time required for a body to stop sliding and transition to roll can be written as follows:

$$t_{roll} = \frac{2}{7} \frac{\left(V_{1to} - V_{2to}\right)}{F_k / m_1} \tag{17}$$

If t_{roll} is greater than the time of contact, then $t_{slip} = t^*$; otherwise, $t_{slip} = t_{roll}$. Rolling resistance is extremely small compared to sliding resistance and hence, for the period of time involved, it is assumed that there is little change in the relative tangential velocity on account of rolling.

Next, the initial and final normal relative velocities are related by the normal coefficient of restitution e, viz.,

$$\left(V_{1n} - V_{2n}\right)_{final} = e \cdot \left(V_{1n} - V_{2n}\right)_{initial} \tag{18}$$

The value for the normal coefficient of restitution is treated as a parameter, since no reliable data are available.

In the case of impact with a rotating spinner, a centrifugal acceleration becomes imposed on the impacting hailstone. The period of time for action of this force may be assumed to be a fraction

of the contact period. The resulting velocity increment due to this acceleration may be estimated as follows:

$$\left(V_{1n} - V_{2n}\right)_{final} - e \cdot \left(V_{1n} - V_{2n}\right)_{initial} = \omega_s^2 R_s t * \frac{1}{F} \tag{19}$$

where, ω_s and R_s are the angular velocity and the radius of the spinner, respectively, at the impact point, and 1/F denotes the fraction of time over which the centrifugal action applies.

2.2.3 Melting and Sublimation.

The two processes (i) conduction, convection, and melting, and (ii) sublimation may be considered as follows. The heat transfer $\dot{Q}_{CC}$ between a hailstone at the temperature T_h and the surrounding air at temperature T_a due to conduction and convection processes is given by the following expression:

$$\dot{Q}_{CC} = -1.68\theta K_a \, \mathrm{Re}^{\frac{1}{2}} \, D\left(T_h - T_a\right)\gamma\chi \tag{20}$$

where θ is a roughness factor, Re, the particle Reynolds number, γ, the surface ratio of a spheroid to a sphere, and χ, the heat transfer factor for a spheroid (reference 3). For a smooth, spherical hailstone, the values of χ, γ, and θ, are all unity. As an example, for a diameter of 2.5 cm with K_a and T_a equal to 0.29 W/mk and 278°K respectively, the thickness of the film formed is 1.3 μ, thus extremely small, although it is adequate to wet the hailstone. It can therefore be assumed that the film may not affect the motion of the hailstone, while it needs to be taken into account insofar as the possibility of (i) freezing on a metal surface and (ii) rolling following impact on a surface.

Sublimation, by which hail goes directly from the solid phase to the vapor phase by diffusion, occurs when the temperature of the hail is less than 273.15°K. The saturation vapor pressure around the hailstone and the relative humidity also play an important part. If the air is fully saturated, there is a negligible amount of sublimation. The heat transfer due to sublimation, $\dot{Q}_S$, is given by the following expression:

$$\dot{Q}_s = -C\theta D_{wa} T_a^{-1} \, \mathrm{Re}^{\frac{1}{2}} \, D\left(1 - R_h\right) E_{sh} \gamma\chi \tag{21}$$

where the dimensional constant C is equal to 9839.45°K and is related to the latent heat sublimation, and D_{wa} and E_{sh}, the diffusion constant and saturation vapor pressure around the hailstone, respectively, are given by the following relations:

$$D_{wa} = 2.302 \frac{P_0}{P}\left[T_a + T_h / 2T_0\right]^{1.81} \tag{22}$$

$$E_{sh} = a \log 10\left(A - \frac{B}{T_h}\right) \times 10^5 \qquad (23)$$

where A and B are estimated from experimental data to be 5.969, and 2224.4, respectively, and the reference values T_O and P_O are taken to be 256°K and 98000 Pa (reference 4). As an example, for a relative humidity of 0.8, T_a equal to 278°K, and T_h equal to 253°K, the thickness of a hailstone of 2.5 cm diameter converted to vapor by sublimation is 2.25 μm/s. Thus, the sublimation is small.

2.2.4 Hail Adhesion.

Adhesion is primarily determined by the freezing of the thin film formed due to melting and impact processes over the time of contact. As the time of impact is very short, usually of the order of microseconds, the temperature of the hail particle and the surface may be assumed to be constant during the time of contact. The thickness of water film that would freeze during the time of contact is given by the following relationship:

$$\Delta h = \left[K_w \Delta T t^* / \rho_w L_f\right]^{0.5} \qquad (24)$$

where Δh is the thickness of the water film, ΔT, the temperature difference between the hail and the surface, with the surface being colder than the hail, and t*, the time of contact.

For a relative velocity of 100 m/s between air and hail, a latent heat of melting of 333.34 kJ/kg-K, hail density of 917 kg/m^3, and a hail temperature of 273.15°K, with an air temperature 5°C above the hail temperature, and a hailstone diameter of 2.5 cm, the thickness of the film formed over a period of 10 ms (roughly, the residence time of a hailstone in a typical large engine inlet) can be estimated form Eq. (21) to be 1.3 μm. Assuming K_w = 0.552 W/m K, ΔT = 20 K, and t* $\approx$ 1 μs, from equation (24) one can estimate the value of the thickness of the frozen layer to be about 0.1 μm. Thus, in the time of contact, only about 10 per cent of the total film thickness can freeze. Such a thin film may not be able to retain the hailstone attached to the impacted surface, noting that it is subject to air-shear and also rolling and rebound, except possibly at the junction of two metal surfaces, such as the root corner of a fan blade.

2.2.5 Break-Up.

Hail stones on impact with each other or with a hard boundary surface may suffer rupture. A simple criterion for rupture is that the stress generated on impact over the contact surface exceeds the permissible value of compressive stress of the materials involved in the impact. In the case of hailstones, two main complexities in determining the stress on impact are (i) the variety of shapes in which a hailstone may appear; and the consequent variation in impact surface area, and (ii) the layered structure of a hailstone with unknown inclusions of solid and other (liquid or gaseous) phase material. Regarding the latter, no data are available on the tensile strength values of a "typical" hailstone or of the material forming the outer solid layer of a hailstone. However, the following illustrative example on the impact of a homogeneous (but noncrystalline) ice particle

provides a basis for estimating the possible rupture of hailstones on impact. The compressive strength is estimated to be in the range 2.5 - 12.5 MPa[25], noting that ice is not a substance with a single set of characteristic features. Considering a particle of ice that impacts a surface of a material such as an aluminum alloy, one can visualize several types of contact: (i) the particle being perfectly spherical and hence, giving rise to a "point" contact of negligibly small area, while at the same time having a strong tendency to slide and roll over the surface, thus possibly escaping rupture; (ii) the particle having a large radius of curvature over the impacting surface, including the case of such impacting surface being flat; and (iii) the particle undergoing impaction at a "corner" or edge of small radius of curvature. In cases (ii) and (iii), the actual contact surface area becomes larger than the impact surface area, the difference being a function of the density of the hailstone and the tensile strengths of the hailstone and the impacted surface material. It is clear that in case (iii) there is the greatest probability of a rupture, although an initial crack over some part of the stone needs to progress sufficiently inwards before a stone falls apart. In this connection, one of the chief unknowns is the internal structure of a hailstone, for example, the thickness of the various layers making up a hailstone.

From Eqs. (4)-(14), and from dimensional analysis, the contact area A and the contact force P can be expressed as functions of the following parameters:

$$A \propto \left(E_r\right)^{-0.4}\left(V_{1n} - V_{2n}\right)^{0.8}\left(R_1\right)^2 \tag{25}$$

$$P \propto \left(m_1\right)^{0.6}\left(E_r\right)^{0.4}\left(V_{1n} - V_{2n}\right)^{1.2}\left(R_1\right)^{0.2} \tag{26}$$

The impact stress, σ_C, is written in terms of the dimensional quantities as

$$_c = \left(m_1\right)^{0.6}\left(E_r\right)^{0.8}\left(V_{1n} - V_{2n}\right)^{0.4}\left(R_1\right)^{-1.8} \tag{27}$$

The compressive strength is estimated to be in the range 2.5 - 12.5 MPa (reference 5), noting that ice is not a substance with a single set of characteristic features. If the impact stress for a hailstone is greater than the compressive strength, then the hailstone is assumed to have cracked and is flagged appropriately.

As an example, for a hailstone of diameter equal to 2.54 cm, assuming typical values for the Young's modulus, the effect of the radius of curvature of the body on the impact stress produced is shown in table 4 for two values of incident normal velocity namely 1 m/s and 100 m/s. In the low incident velocity case, it can be observed in the table that, if the radius of curvature of the body in the vicinity of the contact point is less than 1.25 cm, there is a great possibility that the hailstone may undergo local cracking since the resulting impact stress is then greater than the compressive strength of ice. In the high incident velocity case, unless the radius of curvature is 10 cm or over, the incident hailstone may break-up. If the area of contact is large, as in the case of large, non-circular hailstone, then the impact stress is smaller and the hailstone may not break-up even for large incident normal velocity.

TABLE 4. EFFECT OF INCIDENT NORMAL VELOCITY AND CONTACT AREA ON IMPACT STRESS

Radius of curvature cm	Incident Velocity			
	1 m/s		100 m/s	
	Area of contact cm^2	Impact Stress MPa	Area of contact cm^2	Impact Stress MPa
0.2	5.77e-04	294.0	23.1e-03	1800.00
0.4	2.30e-03	73.6	9.2e-02	460.0
1.0	1.44e-03	11.7	5.8e-02	74.0
1.25	2.25e-02	7.53	9.0e-0.1	47.0
2.50	9.02e-01	1.88	36.0	11.0
5.00	3.60e-01	0.471	14.4	3.0
10.0	1.44	0.117	5.8e+1	0.8

2.3 MODEL FOR THE APPEARANCE OF HAILSTONES IN THE AIR CAPTURE STREAMTUBE.

The hailstones, by the very nature of their formation, growth, and motion in the atmosphere appear in the air capture streamtube in a random fashion with respect to the following: the size distribution, the number entering the capture streamtube at an instant of time, as well as at various locations in space across the cross-sectional area of the streamtube, and the velocity of individual hailstones. The randomness is expressed in terms of probability for each of the parameters in the HINCOF-I code. An example of describing the randomness in regard to various characteristics is provided in figure 2.

2.4 INGESTION PARAMETERS.

Two parameters chosen to describe the ingestion of hail at the engine face for given atmospheric conditions are as follows:

$$F_{n(\text{e or c})} = \frac{\text{Total Number of hailstones entering engine or core at C}}{\text{Total Number of hailstones entering at O}} \tag{28}$$

and,

$$F_{v(\text{e or c})} = \frac{\text{Total volume of hailstones entering engine or core at C}}{\text{Total volume of hailstones entering at O}} \tag{29}$$

where the subscripts e and c denote the engine face and the core face, respectively. The stations O and C are defined in figure 1.

2.5 NUMERICAL PROCEDURE.

A numerical scheme has been developed to develop hail ingestion into an engine inlet while accounting for the main processes during ingestion and is called the HINCOF-I code. The hail stones are introduced at the station O-O (defined in figure 1) with properties like velocity, radius, and frequency of entry chosen from the distributions given in figure 2. At station O-O, the hail particles have equal chances of appearing anywhere in the y direction. Hailstones are introduced in batches at station O-O and can range from 0 to 3 hailstones per batch. The frequency of entry denotes the time interval between entry of fresh batches. A fourth-order Runge-Kutta time stepping scheme is used to solve equations (1) and (2) and advance the hailstones in each time step. All of the other processes discussed earlier are also accounted for during the motion of the hailstones.

The air flowfield is computed first from one of the two methods discussed in appendix A for a particular spinner shape and inlet geometry and specified engine operating conditions. The solution at all of the nodes of the computational grid is thus the known input to the HINCOF-I code. The HINCOF-I code requires as input a number of other quantities that are specific to a simulation and are described in detail in the test case later in this report. This input file is read in at the start of the simulation. Next, the variables in the program are initialized and the simulation is started. The program proceeds in the following order:

i. The hailstones are introduced in batches at the free stream station with their size, velocity, frequency of entry and location of appearance being chosen randomly from given probability density functions for each of the quantities.

ii. These hailstones are advanced by a global time stepping Runge-Kutta method, with their new positions and velocities computed at the end of each time step.

iii. The heat transfer processes undergone by each of the hailstones is computed wherever applicable. The amount of mass lost due to melting or sublimation processes is also computed.

iv. The hailstone trajectory may lead to collisions with other hailstones or with one of the inlet surfaces. This possibility is checked for, and if necessary, the impact processes are handled for each hailstone undergoing impact.

v. The hailstone suffers aerodynamic drag, and hence the air flowfield velocity must be computed at the hailstone location. Since the air flowfield solution is available only at the nodes of a computational grid, the velocity of air at the position of the hailstone must be interpolated from these nodes. This interpolated velocity is then used in the equation of momentum balance for the drag suffered by each hailstone.

vi. Each hailstone is then checked to see if it crosses the engine face, and if so, in which part of the engine face. For each hailstone that crosses the engine face, appropriate flags are set in the program; and,

vii. the fraction of hail entering by volume is checked after each simulation to check for convergence; if convergence is reached, the program calls the output function to write out the results and terminate.

A Monte-Carlo procedure has been used in the HINCOF-I code. This requires a criterion on the basis of which a converged simulation can be assured. The convergence criterion used in this study is the fraction $F_{v(e)}$ for the engine face, defined earlier in equation (29). For the Monte-Carlo procedure, two parameters are defined as follows:

$$F_{v(e1)} = \frac{\sum_{i=1}^{NS} \text{Volume of hailstones entering at engine face / simulation}}{\sum_{i=1}^{NS} \text{Volume of hailstones entering at O / simulation}} \tag{30}$$

and,

$$F_{v(e2)} = \frac{\sum_{i=1}^{NS-1} \text{Volume of hailstones entering at engine face / simulation}}{\sum_{i=1}^{NS-1} \text{Volume of hailstones entering at O / simulation}} \tag{31}$$

$F_{v(e1)}$ denotes the fractional volume of hailstones entering the engine over all simulations including the current simulation, while $F_{v(e2)}$ denotes the fractional volume of hailstones entering the engine over all simulations excluding the current simulation. NS is the number of simulations carried out. Each simulation is carried out over a chosen period, for example of the order of about 0.5 seconds. The convergence criterion can then be stated as follows: Writing

$$CF = F_{v(e1)} - F_{v(e2)}, \tag{29}$$

when the parameter CF is within less than 1 per cent of $F_{v(e1)}$, it is assumed that the solution is converged, and the computation is stopped.

2.6 LIST OF VARIABLES.

A listing of variables utilized in the HINCOF-I code is provided in appendix B in alphabetical order.

2.7 DESCRIPTION OF SUBROUTINES.

A flowchart of the numerical scheme is shown in figure 3. The functions employed in the HINCOF-I code are listed in alphabetical order in appendix C.

3. INPUT AND OUTPUT.

The input to the code and the output are presented in this section.

3.1 INPUT.

The HINCOF-I code needs two input files:

i. Input.dat — This file contains the air flowfield solution either from the NASA code or the PARC code. It consists of the location of the grid points and the values of the flow variables at those grid points.

ii. Auxinput.dat — This file contains the flags and parameters needed as input for the HINCOF-I to select a particular simulation. The following is a line-by-line specification of the inputs:

(a) Choice of pdf for the velocity. It can be either i, for low range of hail entry velocity, or ii, for high range of hail entry velocity.

(b) Choice of pdf for the hail entry size. The numerals i, ii, iii, or iv select the corresponding pdf for the size, as shown in figure 2.

(c) The minimum distance of separation between hailstones at entry to prevent overlap. This is used in the function Gety to choose the location of the hailstones at entry. It must be set greater than zero. A typical value would be the radius of the smallest hailstone.

(d) The time of simulation. It must be set greater than 0.5 second below which the random number generator used in the code will not function properly.

(e) The number of hailstones entering per batch. Typical values used are 2 or 3, yielding a hail ingestion rate of between 400 - 700 c c/s. If set greater than 3, it would lead to a higher rate of ingestion.

(f) The seed for the random number generator. It can be any arbitrary sequence of numbers between 5 to 10 digits long.

(g) The convergence factor CF. The simulation terminates when the value of CF is less than or equal to this input. Recommended range of values is between 0.01 to 0.1.

(h) Flag for output of particle trajectories. If set to zero, printing is suppressed, if set to 1, then the particle trajectories are printed to the file XY.dat.

(i) XYN. To limit the size of the file containing the particle trajectories, the particle position is written every xyn-th time. The recommended intervals are 25 to 100.

(j) Flag for graphical representation on a UNIX workstation. If set to one, an animated image of the simulation is provided on a UNIX workstation running Xwindows, if set to zero, no such animation is generated.

(k) The normal coefficient of restitution rn. The recommended range of values for this parameter is from 0.75 to 1.0.

(l) Flag whether to include heat transfer for the purpose of the simulation. If set to zero, it is not included, while a value of one includes those processes.

(m) Hail entry temperature. It can take values between 243.15°C and 273.15°C, or others as desired.

(n) Flag indicating presence of cross-flow. If set to one, results are presented for the top half and the bottom half of the inlet separately. If set to zero, the results presented are for both the halves combined.

(o) Flag indicating type of spinner. It can be either C or E standing for conical or elliptic spinners respectively. This is used only to print the appropriate title for the output file.

3.2 OUTPUT.

The output obtained consists of the following:

i. The overall ingestion parameters, Fne, and Fve.

ii. The ingestion parameters over any part of the engine face, for example the core section or the bypass section.

iii. The number of hailstones that suffer collisions with other hailstones in passage through the air.

iv. The number of hailstones that impact the inlet surfaces and the frequency with which they do so.

v. The angular velocity imparted to the hailstones due to rolling on impact.

vi. The trajectories of the hailstones through the inlet and surrounding atmosphere.

vii. The amount of melting or sublimation that each hailstone undergoes.

viii. The number of hailstones that suffer break-up due to impact with the inlet surfaces.

The output of the simulation is written to the file Output.dat. This file contains the information for each calculation trial, the number for a trial denoted by N: For the hailstone, its initial size, radius in m, and its initial velocity in m/s; the number of hailstones entering at the engine face, E, the number of hailstones entering the core, C, the number of hailstones undergoing impact in the passage, P, the number of hailstones undergoing impact at a wall surface, W; and the final rotation velocity of a hailstone in rad/s. Also the final ingestion parameters for the whole simulation are printed at the end. A convergence history of the simulation is written to the file Conv.dat. If selected, the file XY.dat contains the trajectories of all the hailstones and can be used for plotting. The following output variables pertain to the above results:

i. Fne, Fve
ii. Fnc, Fvc
iii. collision
iv. wall
v. Omega
vi. Xp, Yp
vii. R, Temp
viii. Impact

4. ILLUSTRATIVE CASE.

A number of cases of ingestion have been computed for illustration of the possible uses of the HINCOF-I code.

The properties of hail utilized in these calculations are given in table 5.

TABLE 5: HAIL PROPERTIES FOR ILLUSTRATIVE CASES

Property	Value
Compressive strength, MPa.	2.5
Youngs' Modulus, GPa.	9.09
Coeff. of kinetic friction	0.02
Density, kg/m^3	850
Latent heat of sublimation, J/kg	2558.2
Latent heat of fusion/melting, J/kg	333.35
Specific heat capacity, J/kg/K	210.16
Thermal conductivity, W/m/K	2.22

The details of the illustrative cases are given in table 6. Among those cases, case I is treated as the basic case, and the use of the HINCOF-I code is discussed for that case in detail in section 4.1. The results of all of the cases are discussed in section 4.2.

TABLE 6. ILLUSTRATION CASES

Group No.	Spinner Shape	Hail Size	Hail Vel.	Hail Temp°C	Inlet Operating Condition	Crossflow Per Cent	Inlet Size
IC	C	(ii)	(i)	0	A	0.0	100 per cent
IE	E	(ii)	(i)	0	A	0.0	100 per cent
IIC	C	(i),(iii)	(i)	0	A	0.0	100 per cent
IIE	E	(i),(iii)	(i)	0	A	0.0	100 per cent
IIIC	C	(ii)	(ii)	0	A	0.0	100 per cent
IIIE	E	(ii)	(ii)	0	A	0.0	100 per cent
IVC	C	(ii)	(i)	-30	A	0.0	100 per cent
IVE	E	(ii)	(i)	-30	A	0.0	100 per cent
VC	C	(ii)	(i)	0	B	0.0	100 per cent
VE	E	(ii)	(i)	0	B	0.0	100 per cent
VIC	C	(ii)	(i)	0	A	3.5	100 per cent
VIE	E	(ii)	(i)	0	A	3.5	100 per cent
VIIC	C	(ii)	(i)	0	A	0.0	80 per cent
VIIE	E	(ii)	(i)	0	A	0.0	80 per cent
VIIIC	C	(iv)	(i)	0	A	0.0	100 per cent
VIIIE	E	(iv)	(i)	0	A	0.0	100 per cent
IXE	E	(iv)	(i)	0	D	0.0	100 per cent

Note:
(1) The hail size and velocity are given with reference to figure 2.
(2) The inlet operating conditions is given with reference to table 3.

4.1 THE BASIC ILLUSTRATIVE CASE.

The shape of the spinner in the inlet can be conical (denoted by C) or elliptical (denoted by E).

The hailstone characteristics, namely characteristic size, location of appearance, frequency of appearance, and velocity, are specified in terms of probability distribution functions given in figure 2. It may be observed that insofar as the size of hailstones is concerned, four distributions are given under (i) to (iv) in figure 2, (i) corresponding to small hail, (ii) to medium sized hail, (iii) to large hail, and (iv) to medium sized hail with the distribution reversed in relation to (ii). Also, regarding the velocity of hailstones at entry to the air capture streamtube, two values have been specified in figure 2, namely (i) being the lower value and (ii) the higher. Finally, figure 2 includes a distribution function for the time interval between successive appearance of hailstones in the entry plane of the air capture streamtube.

The temperature of the hailstone at entry is chosen to be one of two values, namely 0°C or 30°C.

The air flow conditions in the inlet are determined by chosen engine operating conditions and are given in table 3.

4.1.1 Input.

A convergence factor of 0.01 is specified for this illustrative case.

The air flowfield solution is first obtained from one of the two methods outlined in appendix A. The file Input.dat is generated by solving the airflow for the above flight conditions, and the Auxinput.dat file for the HINCOF-I code on page 19.

4.1.2 Output.

The file conv.dat for the simulation begins on page 19.

A listing of the file Output.dat is provided beginning on page 20.

Auxinput.dat file

```
1
3
0.002
1.0
2
84577832
0.01
0
100
0
0.9
1
243.15
0
E
```

Conv.dat file

Convergence History

No.	Fve	Deltav
1	Fv= 0.0000	Deltav=0.5150
2	Fv= 0.5150	Deltav=0.1064
3	Fv= 0.6214	Deltav=0.0873
4	Fv= 0.7087	Deltav=0.0301
5	Fv= 0.7388	Deltav=0.0288
6	Fv= 0.7676	Deltav=0.0096

Fne=0.7612
Fve=0.7774
Fnc=0.2210
Fvc=0.2188

Output.dat file
Elliptic Spinner

N	Radius (m)	Velocity (m/s)	E	C	P	W	Omega (rad/s)
0	0.01250	26.33845	1	0	0	1	-118.717824
1	0.01000	35.11794	1	0	0	3	-200.087367
2	0.01250	35.11794	1	0	0	1	142.936508
3	0.00500	26.33845	1	0	0	1	-337.128301
4	0.01000	0.00000	1	0	2	3	-106.840297
5	0.01000	0.00000	1	0	1	1	-128.720175
6	0.01250	8.77948	1	0	1	0	0.000000
7	0.00200	26.33845	0	0	1	0	0.000000
8	0.01250	26.33845	0	0	0	1	-313.700941
9	0.00200	17.55897	1	0	0	1	-992.121086
10	0.01250	8.77948	1	0	2	0	0.000000
11	0.00500	43.89742	1	1	0	1	-477.646760
12	0.01000	35.11794	1	0	2	1	206.372840
13	0.01250	17.55897	1	0	1	0	0.000000
14	0.01250	0.00000	1	0	0	1	-8.925153
15	0.01250	17.55897	1	0	0	1	86.686334
16	0.00500	35.11794	1	1	0	11	10.941296
17	0.01250	17.55897	1	0	0	0	0.000000
18	0.01250	8.77948	1	0	0	1	-85.111065
19	0.01250	9.77948	1	0	0	1	69.143601
20	0.00200	17.55897	1	1	0	0	0.000000
21	0.01250	26.33845	1	0	0	1	113.894245
22	0.00500	26.33845	1	1	0	0	0.000000
23	0.00500	43.89742	1	1	0	1	-477.646760
24	0.01250	0.00000	1	0	0	0	0.000000
25	0.00500	0.00000	1	0	0	0	0.000000
26	0.00500	43.89742	1	0	0	1	460.484305
27	0.01000	0.00000	1	0	0	2	-157.489609
28	0.00200	26.33845	1	0	0	1	-1083.093057
29	0.00500	8.77948	1	0	0	1	-276.655380
30	0.01250	0.00000	1	0	1	1	-84.926518
31	0.01000	26.33845	1	1	0	1	148.449181
32	0.01000	8.77948	1	0	0	1	-112.257818
33	0.01000	43.89742	1	0	0	1	221.092091
34	0.01000	43.89742	1	0	0	1	-227.185397
35	0.01250	0.00000	0	0	1	1	0.000000
36	0.00200	8.77948	1	0	0	4	-1378.801985
37	0.00200	8.77948	1	0	1	1	-965.820028
38	0.01250	8.77948	1	1	0	0	0.000000
39	0.01250	43.89742	1	0	1	0	0.000000
40	0.00500	26.33845	1	0	0	1	-349.680734

N	Radius (m)	Velocity (m/s)	E	C	P	W	Omega (rad/s)
41	0.01250	8.77948	1	0	0	1	61.160048
42	0.00200	43.89742	1	1	0	1	1275.558889
43	0.0100	8.77948	1	0	0	1	-108.039859
44	0.01250	35.11794	1	0	0	0	0.000000
45	0.00200	43.89742	1	0	0	1	1250.497661
46	0.00500	17.55897	1	0	0	1	278.978260
48	0.01250	35.11794	1	0	0	3	-147.995624
49	0.01000	17.55897	1	0	0	0	0.000000
50	0.01000	26.33845	0	0	0	1	-362.174223
51	0.01250	26.33845	1	0	0	1	113.894245
52	0.00500	0.00000	1	0	0	1	207.042488
53	0.01000	17.55897	1	0	0	1	106.905537
54	0.01000	0.00000	0	0	0	0	0.000000
55	0.01000	43.89742	1	0	0	1	-227.692392
56	0.01250	43.89742	1	0	0	1	-180.491611
57	0.01250	26.33845	1	0	0	1	115.157996
58	0.00500	35.11794	1	1	0	0	0.000000
59	0.01250	43.89742	1	0	0	1	175.220354
60	0.01000	17.55897	1	1	0	1	-124.310857
61	0.00500	26.33845	1	0	0	1	-349.678757
62	0.00200	26.33845	0	0	0	1	-2586.565587
63	0.01000	17.55897	1	0	0	0	0.000000
64	0.00500	43.89742	1	0	0	0	0.000000
65	0.00500	8.77948	1	0	0	0	0.000000
66	0.01250	26.33845	1	1	0	1	-125.484970
67	0.00500	8.77948	1	0	0	1	-258.636256
68	0.00500	17.55897	1	1	0	4	185.868151
69	0.00500	35.11794	1	0	0	1	-409.334923
70	0.01250	8.77948	1	0	0	0	0.000000
71	0.01000	43.89742	1	0	0	1	-230.207210
72	0.00200	8.77948	1	0	0	0	0.000000
73	0.01250	8.77948	1	0	1	0	0.000000
74	0.00500	17.55897	1	1	1	3	-294.998442
75	0.00500	26.33845	0	0	0	4	496.852763
76	0.01250	8.77948	1	0	0	1	60.666744
77	0.01250	17.55897	1	0	0	0	0.000000
78	0.00500	26.33845	1	1	0	0	0.000000
79	0.01250	8.77948	1	0	0	1	64.913178
80	0.01250	8.77948	1	0	0	0	0.000000
81	0.00500	26.33845	1	1	0	1	-95.921471
82	0.01250	26.33845	1	0	0	1	110.343664

N	Radius (m)	Velocity (m/s)	E	C	P	W	Omega (rad/s)
83	0.01250	17.55897	1	0	0	0	0.000000
84	0.01250	26.33845	1	0	0	1	113.894245
85	0.00500	26.33845	1	1	0	0	0.000000
86	0.01250	35.11794	1	0	0	1	-149.605026
87	0.01250	43.89742	1	1	0	1	175.764876
88	0.00500	17.55897	1	0	0	0	0.000000
89	0.01250	43.89742	1	0	0	0	0.000000
90	0.01000	26.33845	1	0	0	0	0.000000
91	0.01000	35.11794	1	0	0	0	0.000000
92	0.01000	43.89742	1	0	0	0	0.000000
93	0.00500	0.00000	1	0	0	1	203.256074
94	0.00200	8.77948	1	0	0	0	0.000000
95	0.00500	17.55897	1	1	0	1	293.101075
96	0.01000	8.77948	1	0	0	1	-103.531688
97	0.00500	17.55897	1	0	0	1	-291.635187
98	0.01250	43.89742	1	1	0	0	0.000000
99	0.00500	17.55897	1	0	0	0	0.000000
100	0.01000	0.00000	1	0	0	1	-98.160975
101	0.01000	0.00000	1	0	0	0	0.000000
102	0.01250	35.11794	1	0	0	0	0.000000
103	0.00500	43.89742	1	0	0	1	457.360711
104	0.01000	0.00000	1	0	0	0	0.000000
105	0.00200	8.77948	1	0	0	0	0.000000
106	0.01000	8.77948	1	0	1	1	-116.228498
107	0.00200	35.11794	1	0	0	1	1116.800581
108	0.00500	43.89742	1	0	0	3	762.065135
109	0.01250	8.77948	1	0	1	3	-243.309201
110	0.01250	26.33845	1	1	1	2	240.245585
111	0.00200	35.11794	1	1	1	2	757.599760
112	0.01250	43.89742	1	1	0	0	0.000000
113	0.00500	0.00000	1	0	0	3	339.193868
114	0.01250	43.89742	1	0	0	0	0.000000
115	0.01250	35.11794	1	0	0	1	143.282809
116	0.00200	17.55897	1	1	0	0	0.000000
117	0.01250	35.11794	1	0	0	1	140.511476
118	0.01000	43.89742	1	0	0	0	0.000000
119	0.01250	26.33845	0	0	0	1	-313.173861
120	0.01000	43.89742	1	1	0	0	0.000000
121	0.01000	35.11794	1	0	0	1	182.174905
122	0.00500	0.00000	1	1	0	2	109.479043
123	0.01250	35.11794	1	0	0	1	143.206998

N	Radius (m)	Velocity (m/s)	E	C	P	W	Omega (rad/s)
124	0.01000	8.77948	1	0	0	1	70.716992
125	0.01000	17.55897	1	0	0	0	0.000000
126	0.00500	35.11794	1	0	0	1	391.561937
127	0.00500	35.11794	1	0	0	0	0.000000
128	0.01000	8.77948	1	0	1	7	-101.832448
129	0.01000	35.11794	1	0	1	8	147.812359
130	0.01250	0.00000	1	1	0	1	60.818388
131	0.01250	35.11794	1	0	0	0	0.000000
132	0.00200	17.55897	1	0	0	0	0.000000
133	0.00500	0.00000	1	0	0	1	203.210538
134	0.01000	35.11794	1	0	0	1	-190.343413
135	0.01250	35.11794	1	0	0	1	-152.293523
136	0.01000	35.11794	1	0	0	1	-189.995044
137	0.01250	26.33845	1	0	0	1	112.202924
138	0.00200	0.00000	0	0	0	1	2136.365112
139	0.01250	17.55897	1	0	0	1	-98.937838
140	0.01000	8.77948	1	0	0	1	-104.374254
141	0.00200	17.55897	0	0	0	1	2350.672075
142	0.01000	43.89742	1	0	0	1	220.682802
143	0.01000	17.55897	1	0	0	2	-161.261560
144	0.00500	26.33845	1	1	0	0	0.000000
145	0.01000	35.11794	1	0	0	0	0.000000
146	0.00500	26.33845	1	0	0	1	318.935702
147	0.00500	8.77948	1	1	0	0	0.000000
148	0.00200	0.00000	0	0	0	2	98.555143
149	0.01000	35.11794	1	0	0	1	182.489157
150	0.00200	17.55897	1	0	0	1	-992.127265
151	0.01250	17.55897	1	1	0	0	0.000000
152	0.00500	43.89742	1	1	0	0	0.000000
153	0.00500	35.11794	1	0	0	0	0.000000
154	0.01000	8.77948	1	0	0	1	81.286059
155	0.01250	43.89742	1	0	0	0	0.000000
156	0.00200	8.77948	1	0	0	1	-928.979631
157	0.00200	17.55897	1	1	0	0	0.000000
158	0.01250	26.33845	1	0	0	0	0.000000
159	0.00500	43.89742	1	0	0	1	459.446313
160	0.00500	35.11794	1	0	0	1	-400.305818
161	0.01000	8.77948	1	0	1	0	0.000000
162	0.01250	35.11794	1	0	1	0	0.000000
163	0.00500	26.33845	1	0	0	8	-575.156717
164	0.01250	17.55897	1	0	0	1	-99.321284

N	Radius (m)	Velocity (m/s)	E	C	P	W	Omega (rad/s)
165	0.01000	26.33845	0	0	0	2	-3.382171
166	0.00200	17.55897	1	1	0	1	840.024007
167	0.01000	26.33845	1	0	0	1	145.497258
168	0.01250	8.77948	1	0	0	2	-51.080656
169	0.01000	26.33845	1	1	0	1	-159.479996
170	0.01250	26.33845	1	0	0	0	0.000000
171	0.00200	8.77948	1	1	0	0	0.000000
172	0.01250	0.00000	1	0	0	0	0.000000
173	0.00500	26.33845	1	0	0	1	-358.875118
174	0.01250	17.55897	1	1	0	3	-107.751054
175	0.00500	0.00000	1	0	0	1	238.813978
176	0.01000	17.55897	1	1	0	0	0.000000
177	0.01000	0.00000	1	0	0	1	72.265154
178	0.01000	0.00000	1	1	3	12	67.990336
179	0.00500	43.89742	1	0	0	1	456.310202
180	0.01250	35.11794	1	0	0	1	143.749868
181	0.01250	43.89742	1	1	0	1	175.765271
182	0.01000	43.89742	1	0	1	2	41.171941
183	0.00200	26.33845	0	0	2	6	-2844.968607
184	0.00200	17.55897	1	0	0	1	-1003.644201
185	0.00200	17.55897	1	1	0	1	993.870339
186	0.00500	0.00000	1	1	0	0	0.000000
187	0.00500	26.33845	1	0	0	1	308.523781
188	0.00500	26.33845	1	0	0	1	308.675735
189	0.01000	26.33845	1	0	0	1	-157.444940
190	0.00200	35.11794	0	0	0	1	2811.651294
191	0.00500	35.11794	0	0	0	1	-1041.046458
192	0.01250	0.00000	0	0	1	0	0.000000
193	0.01000	8.77948	1	0	0	0	0.000000
194	0.01250	43.89742	0	0	1	0	0.000000
195	0.00200	43.89742	1	0	0	1	-1291.421966
196	0.00200	43.89742	1	0	0	6	-324.226835
197	0.00200	26.33845	1	0	0	0	0.000000
198	0.01000	17.55897	1	0	1	1	-123.030995
199	0.00500	0.00000	1	1	1	1	-317.331652
200	0.00500	26.33845	1	0	1	1	-343.683266
201	0.01250	8.77948	0	0	0	1	39.642433
202	0.01000	17.55897	1	0	1	0	0.000000
203	0.01000	0.00000	1	0	0	0	0.000000
204	0.01250	26.33845	1	0	0	1	114.401712
205	0.01000	35.11794	1	0	0	0	0.000000

N	Radius (m)	Velocity (m/s)	E	C	P	W	Omega (rad/s)
206	0.01250	17.55897	1	0	0	1	81.986923
207	0.00500	26.33845	1	1	0	2	158.255809
208	0.00500	43.89742	1	0	0	11	-1247.004238
209	0.01000	26.33845	1	1	0	1	-154.466845
210	0.01000	35.11794	1	0	0	0	0.000000
211	0.00500	0.00000	1	0	0	1	216.021768
212	0.01250	35.11794	1	1	0	0	0.000000
213	0.01000	0.00000	1	0	0	0	0.000000
214	0.00200	8.77948	1	0	0	0	0.000000
215	0.00500	43.89742	1	0	0	1	456.307497
216	0.01000	8.77948	1	0	0	1	-103.935230
217	0.01000	35.11794	1	0	0	0	0.000000
218	0.01000	35.11794	1	1	1	0	0.000000
219	0.00500	35.11794	1	0	1	2	-528.106552
220	0.00500	35.11794	1	0	0	1	-390.567814
221	0.00500	8.77948	1	1	0	1	-262.983054
222	0.00500	26.33845	1	0	0	1	-334.441942
223	0.00500	17.55897	1	1	0	0	0.000000
224	0.01000	26.33845	1	0	0	1	139.347311
225	0.01000	0.00000	1	0	0	1	-98.960220
226	0.01250	26.33845	1	0	0	1	114.907529
227	0.01000	35.11794	1	1	0	0	0.000000
228	0.01000	26.33845	1	1	0	0	0.000000
229	0.01000	35.11794	1	0	0	1	183.110181
230	0.01000	43.89742	0	0	0	1	-568.571059
231	0.00500	0.00000	1	1	0	1	202.757381
232	0.01250	43.89742	1	0	0	0	0.000000
233	0.00500	8.77948	1	1	0	1	-301.311873
234	0.01250	17.55897	1	1	0	0	0.000000
235	0.00200	43.89742	1	0	0	1	1244.057994
236	0.01250	0.00000	1	0	0	1	-73.533749
237	0.00200	17.55897	1	1	0	0	0.000000
238	0.01250	17.55897	1	0	0	0	0.000000
239	0.00500	35.11794	1	0	0	0	0.000000
240	0.00500	35.11794	1	0	0	0	0.000000
241	0.01250	17.55897	1	1	0	8	-49.405135
242	0.01000	17.55897	1	0	0	1	-134.440754
243	0.01250	8.77948	1	1	0	1	70.644450
244	0.01000	17.55897	0	0	0	3	42.356505
245	0.00200	35.11794	1	1	0	0	0.000000
246	0.01250	0.00000	1	0	1	0	0.000000

N	Radius (m)	Velocity (m/s)	E	C	P	W	Omega (rad/s)
247	0.00500	26.33845	1	0	0	1	336.205867
248	0.01000	17.55897	0	0	1	0	0.000000
249	0.01250	35.11794	1	0	0	0	0.000000
250	0.01000	17.55897	1	1	0	0	0.000000
251	0.00200	35.11794	1	0	0	1	-1144.209951
252	0.00200	17.55897	1	0	0	1	2344.913939
253	0.01000	35.11794	1	1	0	1	-194.582254
254	0.00200	0.00000	1	0	0	2	-1099.100204
255	0.01000	8.77948	1	1	0	0	0.000000
256	0.00200	8.77948	1	0	0	0	0.000000
257	0.01000	26.33845	1	0	0	0	0.000000
258	0.01250	43.89742	1	0	1	11	-295.189045
259	0.00200	17.55897	1	0	0	1	-992.119302
260	0.01000	35.11794	1	0	1	0	0.000000
261	0.01000	43.89742	1	0	0	1	217.329544
262	0.01000	17.55897	1	0	0	1	107.221545
263	0.00200	26.33845	1	0	0	1	-1040.673607
264	0.01250	35.11794	1	0	0	0	0.000000
265	0.01000	26.33845	1	1	0	0	0.000000
266	0.00500	35.11794	0	0	0	1	1031.311036
267	0.00200	35.11794	1	0	0	1	1104.458808
268	0.00500	26.33845	1	0	0	0	0.000000
269	0.00200	26.33845	1	1	0	0	0.000000
270	0.00200	35.11794	1	0	0	1	-1088.256217
271	0.00200	8.77948	1	0	0	1	-883.300740
272	0.01000	26.33845	1	1	0	1	139.441159
273	0.01000	17.55897	1	1	0	1	-131.086238
274	0.01000	8.77948	1	0	1	0	0.000000
275	0.01250	0.00000	1	0	1	1	150.167031
276	0.00200	17.55897	1	1	0	0	0.000000
277	0.01250	17.55897	1	1	1	0	0.000000
278	0.01250	43.89742	0	0	1	0	0.000000
279	0.00500	0.00000	0	0	0	1	597.631896
280	0.01250	43.89742	1	1	0	0	0.000000
281	0.01250	43.89742	1	1	0	0	0.000000
282	0.01000	35.11794	1	0	0	1	-186.462163
283	0.00500	8.77948	1	0	0	3	425.472492
284	0.01250	17.55897	1	0	0	1	-96.795547
285	0.00500	35.11794	0	0	0	1	-974.204730
286	0.01250	17.55897	1	1	0	0	0.000000
287	0.01250	0.00000	1	1	1	1	46.513775

N	Radius (m)	Velocity (m/s)	E	C	P	W	Omega (rad/s)
288	0.01000	17.55897	1	0	1	1	117.026843
289	0.00500	8.77948	1	1	0	0	0.000000
290	0.01000	26.33845	1	0	0	2	-211.459201
291	0.01000	8.77948	1	0	0	1	-112.374310
292	0.00200	43.89742	1	0	0	0	0.000000
293	0.01250	17.55897	0	0	0	9	-180.172693
294	0.01250	0.00000	1	1	0	1	59.446738
295	0.00200	8.77948	1	1	0	0	0.000000
296	0.01250	0.00000	1	0	0	1	-76.948068
297	0.00200	17.55897	1	0	0	1	-980.437860
298	0.01000	0.00000	1	0	0	1	-101.760205
299	0.01250	35.11794	1	0	0	1	-150.201282
300	0.01250	0.00000	1	0	0	1	-77.538456
301	0.00200	26.33845	1	1	0	1	1055.704482
302	0.01000	26.33845	1	1	0	1	-161.697118
303	0.00500	26.33845	1	0	0	0	0.000000
304	0.01000	17.55897	1	0	0	1	-131.229446
305	0.01000	43.89742	1	1	0	0	0.000000
306	0.01000	35.11794	1	0	0	1	-192.168351
307	0.00200	26.33845	0	0	0	1	-2596.452387
308	0.00200	17.55897	1	0	0	1	-955.019799
309	0.01250	43.89742	1	0	0	0	0.000000
310	0.01250	35.11794	1	1	0	0	0.000000
311	0.01250	35.11794	1	0	0	1	142.096140
312	0.01250	0.00000	1	1	0	1	-75.243882
313	0.01250	17.55897	0	0	0	1	-234.514702
314	0.01250	26.33845	1	0	0	0	0.000000
315	0.01000	35.11794	1	0	0	1	182.177438
316	0.01250	26.33845	1	1	0	0	0.000000
317	0.01250	0.00000	1	0	0	0	0.000000
318	0.01000	35.11794	0	0	0	1	491.803158
319	0.01250	0.00000	1	0	1	0	0.000000
320	0.01250	0.00000	1	1	1	1	78.255357
321	0.00200	8.77948	1	0	0	1	-928.989282
322	0.01250	17.55897	1	0	0	0	0.000000
323	0.00200	8.77948	1	0	0	0	0.000000
324	0.00500	8.77948	1	0	1	3	-310.270618
325	0.00500	43.89742	1	0	0	1	-474.429139
326	0.01000	26.33845	1	0	1	0	0.000000
327	0.00500	43.89742	1	0	0	0	0.000000
328	0.00500	8.77948	1	0	0	1	247.648823

Fne=0.7612
Fve=0.7774
Fnc=0.2210
Fvc=0.2188

4.1.3 Results.

The calculated values of Fne, Fne, Fve, and Fve are included, along with various other cases in table 7, as cases 1C and 1E. It turns out that for the hail characteristics chosen for this case (as shown in table 5), in the case of the conical spinner about 87 per cent of the ingested particle volume actually appears at the engine face, while 23 per cent of the ingested volume enters the core stream. Thus about 13 per cent of the ingested volume actually becomes diverted away form the engine face. It can also be observed in table 7 that in the case of the elliptic spinner, nearly 33 per cent of the ingested volume becomes diverted away from the engine face, and only about 20 per cent of the ingested volume enters the core. Finally, the fraction of the total number and volume of hailstones entering both the engine face in total and the core are nearly the same; this is largely a function of the medium size of hailstones, type (ii), specified in the example.

TABLE 7. INGESTION RESULTS FOR ALL GROUPS

Group	F_{nc}	F_{vc}	F_{ne}	F_{ve}
IC	0.229	0.218	0.897	0.874
IE	0.2	0.201	0.714	0.672
IIC(i)	0.2475	0.2723	0.922	0.90
IIC(iii)	0.205	0.216	0.785	0.803
IIE(i)	0.354	0.375	0.903	0.873
IIE(iii)	0.162	0.172	0.639	0.651
IIIC	0.202	0.160	0.867	0.841
IIIE	0.186	0.181	0.636	0.595
IVC	0.218	0.226	0.873	0.816
IVE	0.227	0.241	0.755	0.734
VC	0.213	0.202	0.876	0.872
VE	0.196	0.191	0.742	0.667
VIC(top)	0.08	0.97	0.318	0.299
VIC(bot)	0.102	0.102	0.43	0.465
VIE(top)	0.063	0.072	0.188	0.162
VIE(bot)	0.087	0.110	0.475	0.471
VIIC	0.19	0.203	0.890	0.83
VIIE	0.189	0.159	0.634	0.607
VIIIC	0.296	0.264	0.931	0.915
VIIIE	0.361	0.324	0.925	0.90
IXE	0.312	0.338	0.899	0.921

Although not shown here, it is found from an analysis of the motion of hailstones in the test case that a large proportion of hail stones undergoes rolling over the impacted surface following contact, thus gaining angular velocity.

From the hailstones flagged for undergoing collision with other hailstones, it is found that less than 10 per cent of the stones undergo collision.

Lastly, heat transfer to the hailstones does cause some melting, but both heat and mass transfer are relatively small effects.

4.2 THE OTHER TEST CASES.

It can be observed in table 6 that the test cases II through IX differ from the test case I in inlet operating conditions, hail size and velocity distribution, hail temperature, and the pressure of a cross-flow due, for example, to non-zero angle of attack for the inlet.

Based on the predicted results, it can be seen in table 7 that there is substantial variation in the number and volume fraction of hailstones form case to case.

4.2.1 Effect of Shape of Spinner.

The elliptic spinner is found to divert the hailstones away form the engine fare more effectively than in the case of the conical spinner in all but a few cases shown in table 7. The main exceptional cases, noting the probabilistic nature of the results in all cases, are cases (V) and (VI) with an increased velocity of air flow and case (VIII) with medium sized hail distribution but, unlike in case (II), with most of the hailstones being in the smaller sizes. These cases are of considerable interest since they show that combinations of size and velocity distribution can produce substantial differences in the ingestion at the engine face as well as into the core for the case of elliptic spinners, which, thus, may not be universally better than conical spinners. However, the results do indicate that spinner geometry has a substantial effect on the diversion of hailstones, and, therefore, provides a significant design variable.

4.2.2 Effect of Inlet Flow Conditions.

4.2.2.1 Velocity of Air Flow.

Considering cases V and IX with high air flow velocity in relation to the lower air velocity cases, it is found that ingestion of hail at the engine face is in general lower for both the conical and the elliptic spinners. However, as stated earlier, the size distribution of hailstones introduces differences between different types of spinners in both the overall ingestion across the engine face and ingestion into the core stream.

4.2.2.2 Size of the Inlet.

In case VII, the size of the inlet is reduced to 80 per cent of the size for case I while all other air flow and hail characteristics are held constant in the two cases. It is found in case VII that the amount of ingestion at the engine face becomes reduced for both the conical and the elliptic spinner; the decrease being greater in the case of the elliptic spinner. Thus, it appears that the elliptic spinner is particularly effective in the case of small engines; the reason may be that in the smaller inlet there is a greater interaction between the spinner and the inlet wall thus yielding a duct-like flow in which the hailstones also undergo motion and rebound affected more by the boundary walls than by the main flow.

4.2.2.3 Cross-Flow into the Inlet.

One of the common flight regimes for an inlet is operation with an angle of attack relative to the direction of flight. A nonzero angle of attack causes a change in both the capture streamtube area and the motion of air and hailstones inside the inlet. An angle of attack is thus equal to the introduction of a cross-flow, for example one degree of angle corresponding to cross-flow equal to 1.745 per cent of the main flow.

In case VI it is assumed that the inlet operates with a negative angle of attack of 2° arc, all other conditions remaining the same as in case I. It can then be seen in table 8 that the ingestion at the engine face differs between the top and the bottom portions of the inlet. The bottom half of the inlet experiences less ingestion than the top half of the inlet in the case of both the conical and the elliptic spinners; the elliptic spinner does appear to shield the top half somewhat more than the conical spinner. In all cases, there does appear an asymmetry in ingestion at the engine face. At the same time it is noteworthy that the total amount of ingestion at the engine face is less than in case I. In view of this, there is some scope for considering the effect of reorienting the spinner when the inlet is operating in a zero-angle of attack mode to establish if a slight tilting of the spinner has a noticeable effect on ingestion.

4.2.3 Effect of Hail Ingestion Conditions.

4.2.3.1 Size of Hailstones.

Comparing cases I and II, it is found, as shown in table 7, that an increase in the size of hailstones leads to a decrease in the amount of ingestion at the engine face, both in the case of the elliptic and the conical spinners. The larger amount of ingestion in the case of smaller hailstones is, it can be concluded, due to the smaller inertia of such hailstones and the greater tendency to follow the air stream.

4.2.3.2 Size Distribution of Hailstones.

In case VIII, as stated earlier, the size distribution of hailstones is reversed relative to that for case I, all other conditions remaining the same. Then, in case VIII, with the hailstones of smaller size being in larger numbers compared to those of larger size, the amount of ingestion increases for both types of spinners. The same observation was made earlier in the discussion on changing the size of hailstones.

It is significant that when the hailstones are of small size, a simple elliptic spinner is not more effective than a conical spinner. It is possible that a spinner of the shape of a super-ellipse can be more effective in diverting small hailstones away form the engine face.

5. DISCUSSION.

The HINCOF-I code provides for given atmospheric and flight conditions a means of determining hail motion and ingestion through an inlet up to the engine face. The flowfield of air must be determined separately and used as part of the input. A number of characteristics have been identified as significant in accounting for various processes occurring during the ingestion of hailstones. A set of ranges of values for each of the characteristics have been given for use in establishing ingestion at the engine face, and these can be replaced by other values when necessary and available.

The hail motion is determined in a radial plane including the axis of the inlet. In the case of a non-axisymmetric inlet (whether internally or in external shape) it is necessary to perform calculations independently for the radial planes of interest. The code does not account for fully three-dimensional motion. However, the code can be utilized to determine the effect of an angle of attack provided it is confined to a radial plane.

The code requires as input the random variations in size, velocity, and space- and time-wise variations in appearance of hailstones at a suitable, entry plane in the air capture streamtube. The random values can be expressed in terms of probability density functions.

The code utilizes a form of Monte-Carlo procedure for taking account of randomness in inputs. The numerical procedure has been shown to yield converged solutions based on a convergence criterion related to the total volume of hailstones appearing at the engine face for given entry conditions.

In a set of nine cases of ingestion examined as test cases for the use of the HINCOF-I code, it is found that converged solutions can be obtained in six simulations, each simulation conducted over a period of 0.5s.

The predictions obtained for the fractions of the total number and volume of hailstones ingested at the engine face and over the engine core part of that face appear to be reasonable. The code also seems to provide a satisfactory method of determining the influence of various parameters such as the geometrical shape of the spinner, the inlet flow conditions including velocity of air flow, size of the inlet, cross-flow (or angle of attack), and hail ingestion conditions including size of hailstones, and size distribution of hailstones.

There seems to be scope for examining the use of such other shapes as a super-ellipse and also a slight tilting of the spinner axis. It is obviously crucial in all such cases to note the possible effects on other aspects of engine performance.

The test cases for which predictions have been obtained have shown that the ingestion at the engine face is less sensitive to the engine operating conditions than hail entry conditions.

Among the various parameters, the hail size and its distribution have the most dominant effects on ingestion at the engine face.

The test cases have also served to establish the influence of spinner geometry on ingestion at the engine face. It is found that an elliptic spinner is generally better than a conical spinner in diverting hailstones away from streaming into the engine face.

At the same time, it should be noted that there are several cases where the elliptic spinner is not effective, especially when the hail size is small and also, the engine inlet size is large; in the latter case the spinner does not scale linearly with the size of the engine face in practical engines.

The greatest uncertainty in the processes undergone by the hailstones in the course of ingestion is in regard to two factors, namely (i) melting and sublimation during motion and on impact with one another or a material surface and (ii) deposition and pealing without or with break-up following impact on a surface. During contact between hailstones there is also uncertainty in regard to reaccretion and disintegration or shattering. Experimental studies are the only means of obtaining the needed insight in respect of the foregoing (references 6,7,8,9).

6. REFERENCES.

1. Sommerfeld, M., "Modelling of Particle-Wall Collisions in Confined Gas-Particle Flows," *International Journal of Multiphase Flow*, Vol. 18, No. 6, pp. 905-926, 1992.

2. Engel, P.A., "Impact Wear of Materials," Elsevier Scientific Publishing Company, New York, 1976.

3. List, R., and Dussault, J.G., "Quasi Steady State Icing and Melting Conditions and Heat and Mass Transfer of Spherical Hailstones," *Journal of the Atmospheric Sciences*, Vol. 24, pp. 522-529, September 1967.

4. Eckert, E.R.G., and Drake, R.M., "Analysis of Heat and Mass Transfer," McGraw-Hill, New York, 1972.

5. Dorsey, N.E., "Properties of Ordinary Water-Substance in all its Phases: Water-Vapor, Water, and all the Ices," New York, Reinhold Publishing Corporation, 1957.

6. Papadakis, M., Breer, M.D., Craig, N.C., and Bidwell, C.S., "Experimental Water Droplet Impingement Data on Modern Aircraft Surfaces," AIAA Paper No. 91-0445, Reno, NV, 1991.

7. Render, P., Pan, H., Sherwood, M., and Riley, S.J., "Studies into the Hail Ingestion Characteristics of Turbofan Engines," AIAA Paper No. 93-2174, Monterey, CA, 1993.

8. List, R., and Charlton, R.B., "Hail Size Distributions and Accumulation Zones," *Journal of the Atmospheric Sciences*, Vol. 1182-1193, September 1972.

9. List, R., Schuepp, P.H., and Methot, R.G.J., "Heat Exchange Ratios of Hailstones in a Model Cloud and their Simulation in a Laboratory," *Journal of the Atmospheric Sciences*, Volume 22, pp. 710-718, November 1965.

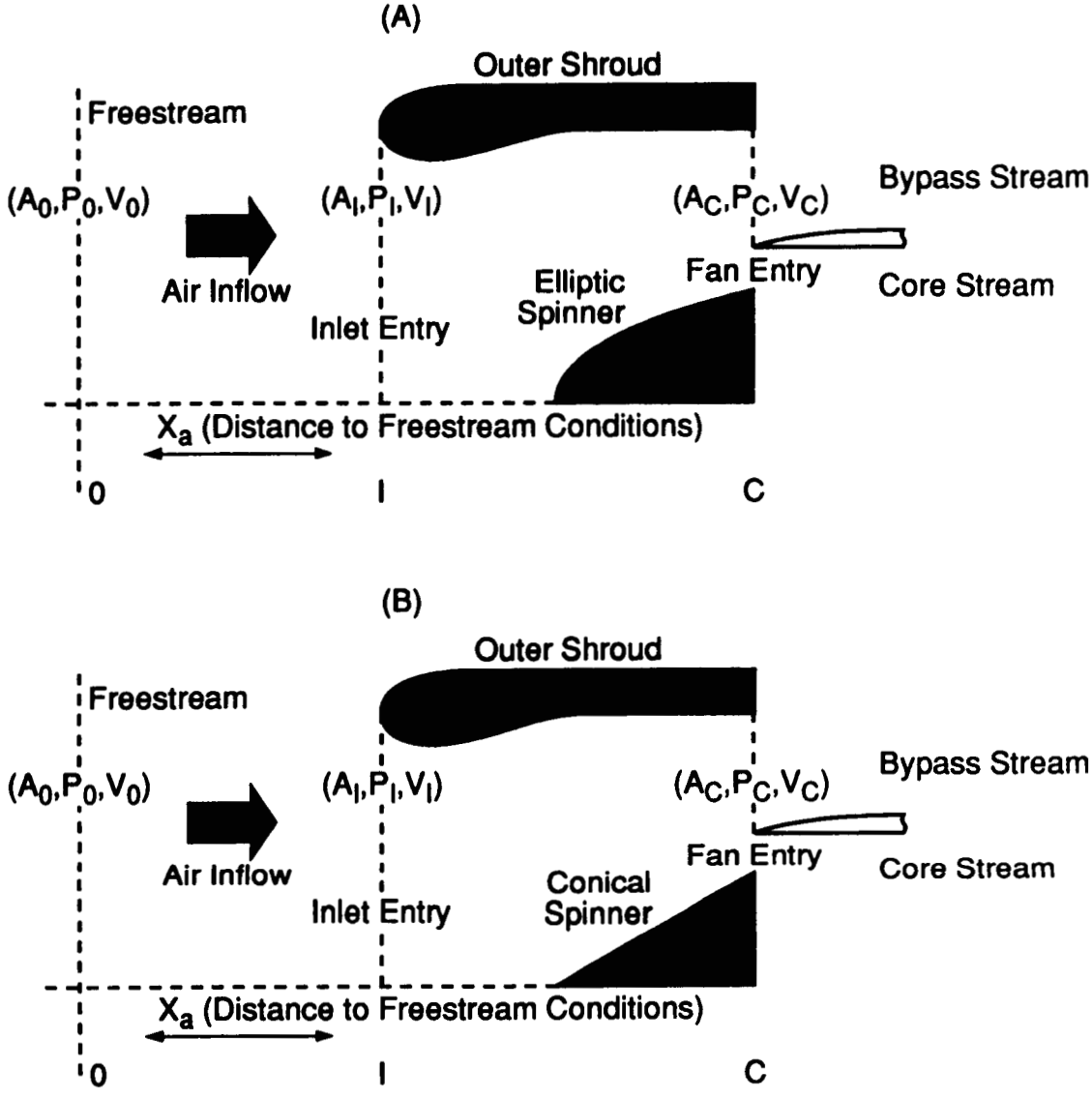

FIGURE 1. SKETCH OF INLET WITH DIFFERENT SPINNERS

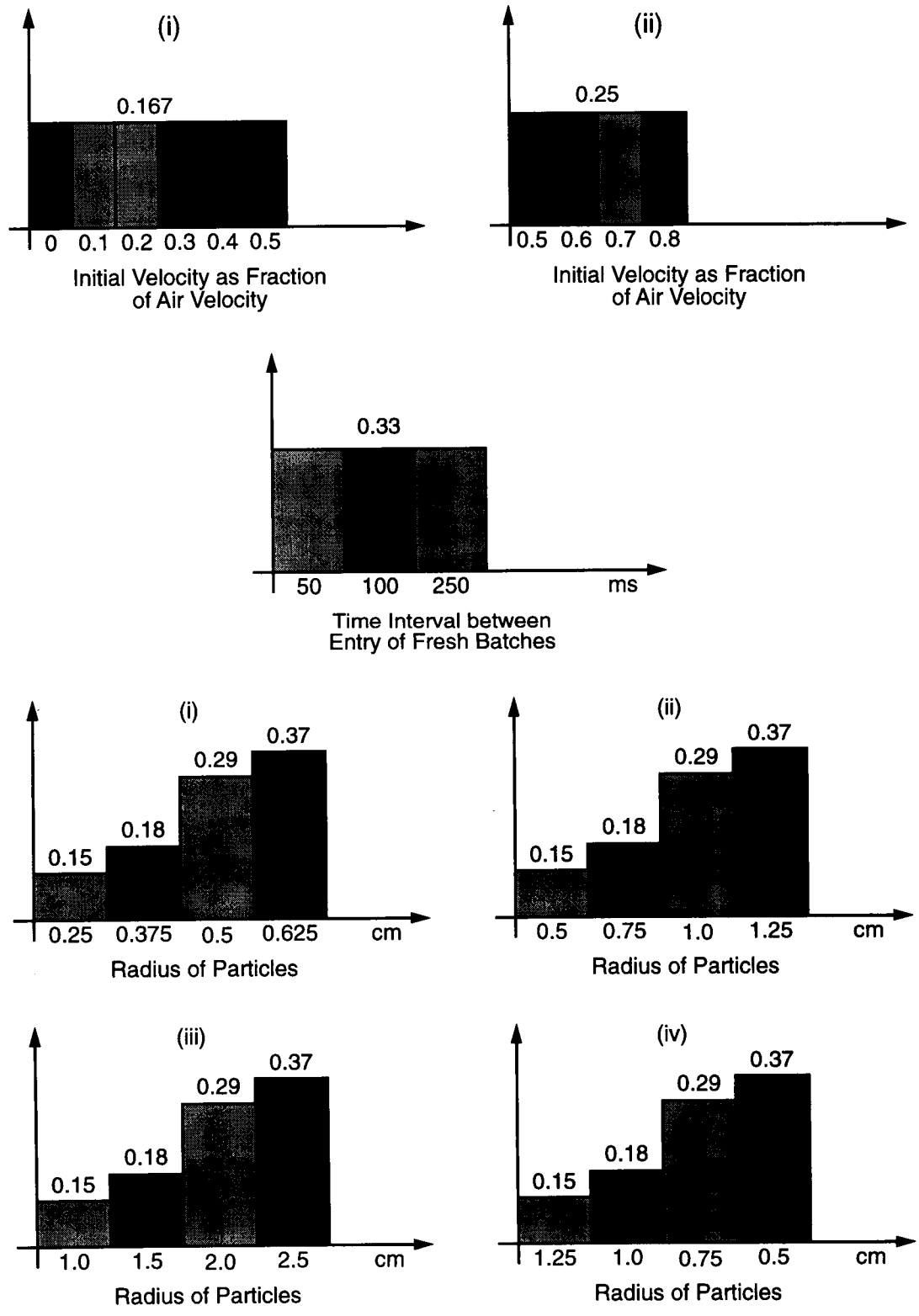

FIGURE 2. PROBABILITY DENSITY FUNCTIONS

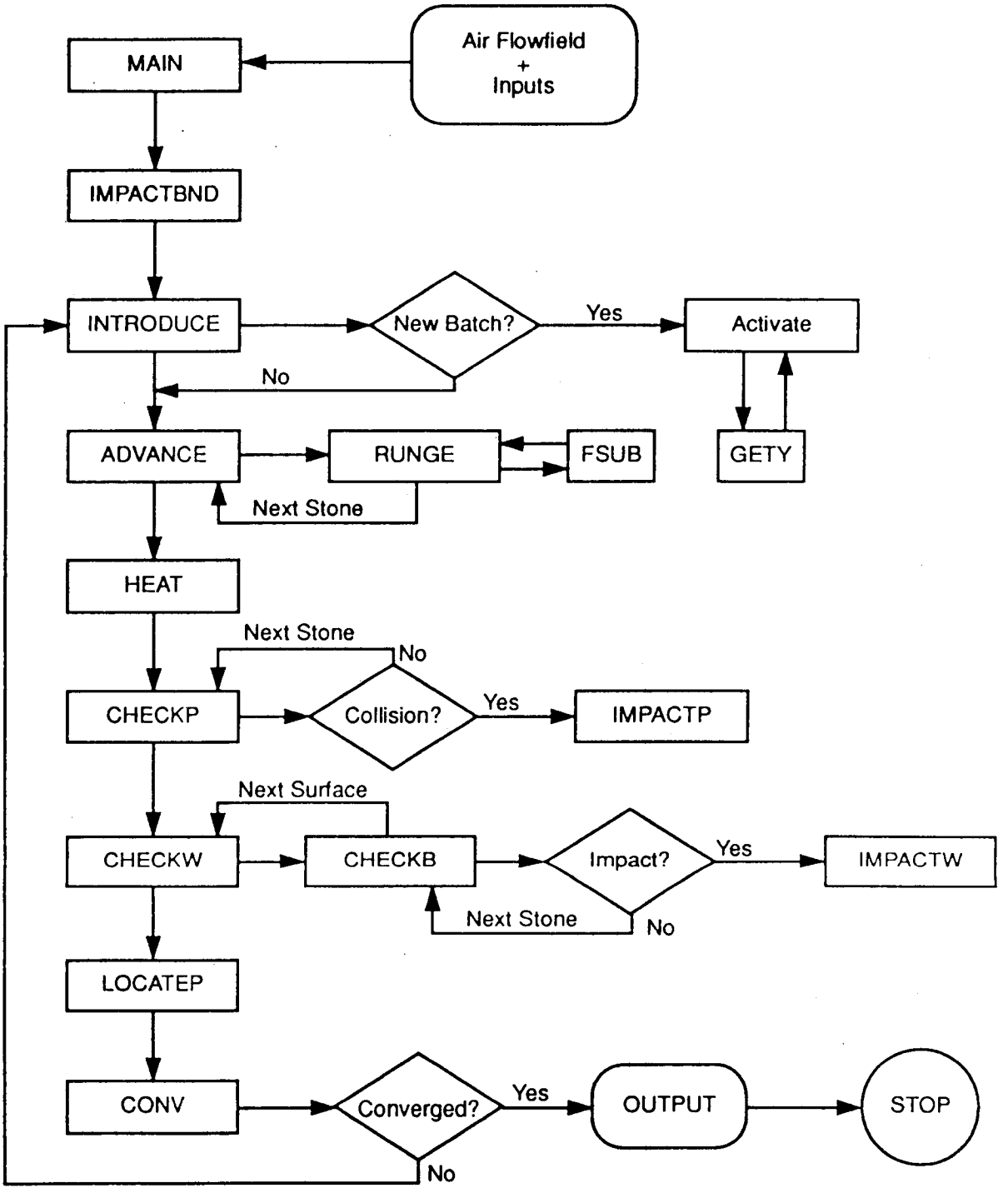

FIGURE 3. FLOWCHART OF THE NUMERICAL SCHEME

APPENDIX A
METHODOLOGY FOR DETERMINING AIR FLOWFIELD OF ENGINE INLETS

1. STOCKMAN CODE.

The set of computer programs used to solve for the flow in an inlet of specified geometry and flight conditions consists of the following basic elements. The chief element is the Douglas program for incompressible potential flow. A program to represent the inlet geometry by analytical contours for input to the Douglas program forms another element. The final element combines the basic incompressible potential flow solution to produce a solution for any combination of mass flow, free-stream velocity, and angle of attack. The combination program incorporates a compressibility correction that can handle local transonic Mach numbers. The viscous flow solution is based on the Princeton method for calculating boundary layers on curved surfaces with routines added to calculate boundary layer transition. The program solves for the flow in an inlet in the following steps (references 1, 2):

1. Geometry representation (Program SCIRL)
2. Incompressible potential flow basic solutions (EOD)
3. Combined solution with compressibility correction (COMBYN)
4. Viscous correction to the solution (BOUNDD)

1.1 SCIRL.

The inlet is assumed to be axisymmetric and is represented by its meridional profile. This profile is broken into segments at convenient tangent points. Each segment may be defined by an analytic expression or a set of points. The inlet duct walls and the outer surface must be extended far downstream to facilitate obtaining accurate potential flow solutions in the inlet regions of interest. The geometry program SCIRL prepares coordinate point input for efficient use of the potential flow program and also prints out information such as curvature, wall angles, flow area distribution, etc., which is useful in preliminary screening of proposed inlet shapes. In addition to the surface points, sets of points spanning the passage, like flow measuring rakes, are needed at axial locations where velocity profiles or streamlines are desired. At least one "rake" must be specified for use as a control station, which is needed by COMBYN. Program SCIRL generates the coordinates of the rake points for input to EOD on unit 17. The points and analytic shapes are specified by an input file on unit 5.

1.2 EOD.

The Douglas Neumann program is used to calculate the incompressible potential flow solution. The program utilizes a large number of sources and sinks of initially unknown strengths on the surface of the inlet. It is assumed that each surface element is a straight line segment and that the source or sink is located at the midpoint of each element. The Douglas axisymmetric potential flow program, denoted by EOD is used to obtain three basic solutions for flow about inlets. These solutions are $\vec{V}_1$, axial flow with inlet duct extension closed, $\vec{V}_2$, axial flow with inlet duct

open, and $\vec{V}_3$, the cross flow solution with the duct extension open. The program takes its input about the shape of the inlet from the output of SCIRL, on unit 5. It writes the solution to unit 7.

1.3 COMBYN.

This program combines the three basic solutions into a solution of interest that can be expressed as:

$$\bar{} = A\vec{V}_1 + B\vec{V}_2 + C\vec{V}_3$$

The combination coefficients A, B, and C are determined by specifying any combination of (i) freestream velocity V_∞, (ii) inlet incidence angle α, and (iii) average axial velocity $\vec{V}_c$ as specified at a control station in the inlet. The control station is a rake of off-body points (points away from the inlet surface) in the inlet. This program also corrects the incompressible potential flow solution for compressibility using the method of reference. Viscous correction is applied through the subroutine BOUNDD which is based on the Herring and Mellor boundary layer program, which solves the partial differential equations of mass, momentum and energy. This method linearizes the partial differential equations by using finite differences for the x derivatives resulting in a series of ordinary differential equations. The ordinary differential equations are then integrated numerically across the boundary layer at each x location. The corrections are then applied to the velocity profile obtained previously in COMBYN. This program reads in input from EOD on unit 7. Two additional input files are needed, one on unit 5 and the other on unit 24 for the COMBYN program. The final input, in terms of the velocities along the rakes, in a form suitable for input to the HINCOF-I code is written to unit 99.

A UNIX batch file has been written to automate this whole process, and can be suitably modified for any other platform.

1.4 INPUT.

Input files for one of the cases are printed below; for a more detailed explanation of all quantities and flags in the input files please refer to the accompanying documentation:

The input file to SCIRL is shown on page A-3.

The input file to COMBYN on unit 24 is shown on page A-4.

1.5 OUTPUT.

A listing of all the velocities at the rake points is written to unit 99 in the order X, Y, V_X, and V_Y to be read in by HINCOF-I.

Input SCIRL

```
                BURLEY1Q
    12.       0.          2.              6          0.          2.

QCSEE1    EOD       1 1
      2.          .40         2.              0.
   25
35.         4.6         10.          32
-15.0       0.          32.          32
-10.0       0.          30.          32
-5.0        0.          25.          32
0.0         0.          15.          32
5.0         0.          13.          32
9.0         0.          11.          32
10.0        0.          10.          32
10.25       0.           9.35        32
10.5        0.           9.          32
12.0        0.           8.42        32
13.00       0.           8.24        32
15.0        0.           8.3         32
16.0        0.           8.36        32
18.0        0.           8.5         32
20.         0.           8.79        32
23.         0.           9.25        32
24.         0.           9.41        32
25.227      0.0          9.53        32
26.         1.65         9.67        32
27.         2.45         9.8         32
28.         3.15         9.88        32
29.         3.65         9.55        32
31.         4.25        10.0         32
33.000      4.55        10.0         32
1.            2.                                 1.0
0.            1.78          1.78
```

Input file COMBYN on unit 24

```
25.227          25.227                                  33.832          35.
-1.             0.                                      4.6             4.6
1.
33.832          90.
4.6             4.6
      2.          7
      1.
     90             33.832
     10.            10.
      1.
   33.832           30.582
     10.            10.
     -3.
     33.832         30.582        13.468                    10.
     10.            10.             8.258                    8.258
     1000.       2.       2.
     14.            13.468                                   10.          10.
     8.258          8.258                                    9.992        11.00
     1000.     2.246      1.767
     10.            10.                                     14.863        16.0
     9.             9.992                                   11.102        11.102

     1.
    14.863        33.832
   11.102         11.102
     1.
    33.832        90.
    11.102        11.102
```

```
            GE2;BURLEY1Q,,READING 3097 BLOWING
 259 800 259 800                    -2
  0       0.      0.      0.     12.                                    0000     24.000
2116.    518.67  0.00     .01     0.000   0.300   0.100
   1   1  32   0   0   1
 180.0
35.000    0.0000    10.000
10.000    0.000     9.992     60
 &PARAMS LABEL=' TRY2',&END


&INPUT ALFA=00 0,NLEW=1,lewscp=0,&END
```

2. PARC CODE.

The PARC code is a flow field simulation program that calculates the thermodynamic and kinematic properties of a fluid flow at discrete points within the flow, based on a specified boundary geometry and appropriate flow conditions on these boundaries. The boundaries can be quite complex, and the fluid can be treated fairly generally. Inviscid and viscous flows can be calculated. Viscous flows can be laminar or turbulent and can be treated as fully viscous or as shear layer flows. Turbulent flow is calculated by considering the Navier-Stokes equations as having been Reynolds-averaged (mass averaged) and by using an algebraic turbulence model to determine a turbulent viscosity. The viscous coefficients are determined from Sutherland's viscosity law, Stokes hypothesis, and an assumption that the Prandtl number is constant. This code has been optimized as a steady state flow solver.

The basis of the algorithm used in the PARC code is the complete Navier-Stokes equations in conservation law form. That is, the divergence form of the time-dependent continuity, momentum, and energy equations is the heart of the physics modelled in this code. The Beam and Warming approximate factorization is the basis of the algorithm. This algorithm is an implicit scheme that solves the set of equations produced by central differencing the Navier-Stokes equations on a regular grid. Since these equations are formulated in the strong conservation form for a curvilinear set of coordinates, the resulting algorithm is quite general with the desirable features of global conservation and shock capturing (reference 3).

2.1 USAGE.

2.1.1 Program Exeuction.

The submit file, batch job file, or job control file (whichever is preferred) must make available appropriate input files and compile, load, and execute the code and store the output files. This file is not provided as part of this code for all platforms currently. It is provided only for UNIX platforms and can be modified suitably for other platforms. There are two mandatory input files:

a. Restart file (assumed to be assigned to unit 2), which contains the grid information and the old solution.

b. Parameter file (assumed to be assigned to unit 9), which contains the information necessary to:

   1. Specify completely the problem being solved

   2. Control program execution

   3. Select desired input and output options

2.1.2 Output Files.

Two output files are always created, and one optional output file can be produced if called for in the inputs. These files are:

a. New restart file (assigned to unit 4), which contains the grid and the just-calculated solution.

b. Run history file (assigned to unit 6), which contains a listing of parameter inputs, convergence information, a printed map of selected portions of the flow field, and diagnostic information.

c. Output file containing flux variables suitable for plotting by PLOT3D. A filter program, also included and called convert, is used to convert the flux variables into primitive variable form. This file is called Input.dat.

2.2 INPUT.

2.2.1 Nondimensionalization.

Since the PARC code is based on a nondimensionalized set of equations, many of the inputs to and outputs from the code are also nondimensional.

2.2.2 Files.

Two input data files are required to execute the PARC code. One, which is the restart file, and is present as fort.2 on UNIX platforms, is the restart file. A sample program to generate the restart file for the set of problems concerned is included with this distribution, called restart.f. This file must be modified appropriately, or a completely new one can be generated to generate the initial conditions and the grid information. They are read by the statements on page A-8 where r represents the value of density, ru represents density times velocity in the x direction, rv represents density times velocity in the y direction, and e represents the total specific energy.

The other file, which is always expected to be on unit number 9, (fort.9), is the parameter file. It provides parameter input to the code consisting mainly of Namelists. They must be in the following order:

INPUTS	List of parameters controlling execution
BOUNDS	Geometry and boundary specification

2.2.3 Flow Equations.

Axisymmetric, inviscid, thin-layer, fully viscous, laminar or turbulent specializations of the Navier-Stokes equations are selected by appropriate use of the following parameters.

a. IAXISY axisymmetric or 2-D form of the Navier-Stokes equations selection parameter. A value of zero for this parameter selects the 2-D form of the Navier-Stokes equations; the axisymmetric form is selected for a value of one (the default).

b. INVISC an integer vector with two (2-D) elements. Each element is paired with a grid index as follows: 1-J, 2-K (e.g., INVISC (2) contains information relating to the K index). A value of one for an element of INVISC causes viscous flux differences to be included for the coordinate direction (e.g., INVISC (2) = 1 causes the difference of the appropriate viscous fluxes at K+1, and K-1 to be calculated at every grid point). Thus the following options:

restart.f. or alternative

```
read (2) (((x(j,k),j=1,jmax),k=1,kmax),
         (((y(j,k),j=1,jmax),k=1,kmax)
read (2) (((r(j,k),j=1,jmax),k=1,kmax),
         (((ru(j,k),j=1,jmax),k=1,kmax),
         (((rv(j,k),j=1,jmax),k=1,kmax),
         (((e(j,k),j=1,jmax),k=1,kmax)
```

1. Inviscid — all elements are zero

2. Thin layer — the element corresponding to the coordinate that varies across the shear layer is set to one; any others are set to zero (e.g., in a 2-D problem for which the K varying lines cross the shear layer, this option is selected by INVISC(1) = 0, INVISC(2) = 1).

3. Fully viscous — all elements are one (the default). For complex viscous flows the last option is recommended.

c. LAMIN — an integer vector whose elements are connected with the grid indices in the same way as INVISC. A value of one for any element of LAMIN causes the flow to be treated as turbulent. Thus the following options:

1. Laminar — all elements equal to zero. This corresponds to a laminar boundary layer computation.

2. Turbulent — any element equal to one. For the algebraic turbulence model used by the PARC code, the elements of LAMIN have to be set in the same fashion as for the thin-layer option for INVISC, to give best results.

2.2.4 Flow Properties.

The simulation fluid and flow properties are set by the following parameters (the default values apply to air at standard conditions):

a. GAMMA — The ratio of the specific heats at reference conditions (Default value is 1.4).

b. PR — Prandtl number at reference conditions.

c. VRAT — Ratio of the second coefficient of viscosity to the first coefficient of viscosity (Default is - 2/3 which is Stokes hypothesis).

d. TREFR — Reference temperature in degrees Rankine.

e. RE — Reynolds number based on the reference density, speed of sound, length, and viscosity. There is no default, must be supplied.

f. PRT — Turbulent Prandtl number (default 0.9).

2.2.5 Grid Dimensions.

a. PARAMETER statements in the PARC code:
NX,NY — Array sizes for the first and second (J and K) indices of the grid and flow-field arrays (e.g., the X-coordinate array is dimensioned as X(NX,NY)). These can be set to JMAX and KMAX or larger values.
NM — The largest of NX or NY.

b. NAMELIST INPUTS parameters:
JMAX, KMAX — Maximum indices for the first and second indices of the grid and flow-field arrays. These parameters, along with the boundary condition parameters, set the DO Loop limits in the PARC code. Thus, JMAX≤ NX, and KMAX≤ NY must always hold true.

2.2.6 Artificial Viscosity.

Since the PARC code uses central differencing, an appropriate level of artificial viscosity is always required. The following parameters can be used to control the amount and type of artificial dissipation:

a. DIS2 — Coefficient of the second-order artificial viscosity. This type of dissipation is very diffusive in general. Its primary purpose is to enhance stability and accuracy in the vicinity of strong shocks and to improve the robustness of the PARC codes during strong transients. An automatic damping coefficient limits the effectiveness of this type of dissipation to regions of the flow that possess significant numerical pressure gradients (e.g., P(J+1, K, L)-(P(J-1, K, L) is large compared to P(J, K, L)). Thus expansions and

compressions that are resolved over a small number of points can trigger an inappropriate amount of this artificial viscosity (only current remedies are to reduce the value of DIS2 and/or regrid for better resolution in these areas). In general, it is recommended that all simulations be started with DIS2 at its maximum value of 0.25 (the default), and then that the value of DIS2 be reduced as low as is consistent with stability and accuracy.

b. DIS4 — Coefficient of the fourth-order artificial viscosity. This type of dissipation is uniformly applied but should have no more effect on the accuracy of the solution than that produced by the inherent errors of the PARC algorithm. Although the DIS2 parameter's value can often be set to zero with minimal effect on stability, the value of DIS4 must almost always be non-zero. For many problems, variation in the value of DIS4 produces negligible differences in the flow field. Thus it is generally recommended that the value of DIS4 be kept at its maximum (0.64, the default). After the value of DIS2 has been reduced as much as possible, reduction of the value of DIS4 can be attempted to note its effect on the simulation. However, as noted above, this is rarely worthwhile.

2.2.7 Output Format.

A number of options are available to control the amount and format of both printed output and output that is intended to be plotted. Convergence history, printed as spelled out in the Output section part of the printed output includes a convergence history that gives the user information on the behavior of the simulation during the course of a run. The amount of this history is controlled by the following parameters:

a. NSPRT — Frequency of convergence history print parameter. For example, if the value of NSPRT were ten (the default value), then the convergence history parameters (e.g., the L_2 residual) are calculated and printed every tenth iteration.

b. IFXPRT — Parameter that allows the inclusion of the flux balance histories. A value of zero (the default) excludes them from the printed convergence history, and a value of one causes the flux balances to be calculated and printed.

c. IPLOT — This option governs whether to generate files suitable for reading by the graphics postprocessor PLOT3D. A value of one (default zero) writes two files fort.31 and fort.30 which contain the flux variable and the grid information respectively, which can then be read by PLOT3D.

2.2.8 Boundary Conditions.

The PARC code is designed so that specification of boundaries and boundary conditions is done entirely through inputs to the program in a very general manner. This makes the use of the code very flexible but requires that boundary specification be a large part of the inputs. As an aid in explaining the function of the boundary parameters, the simple problem laid out in figure A-1 will be used as an example application.

a. Basic Procedure — The methodology to be used in generating the information required to specify the boundary parameters is as follows:

1. Locate and label boundary segments — break the boundaries up into segments so that each segment is (i) contained on a coordinate surface (a J or K constant surface), (ii) made up of contiguous points that can use the same boundary condition information (e.g., each point is a no-slip wall point with the same specified temperature), (iii) distinct from all other segments (i.e., no shared points), (iv) simply connected (i.e., no "holes" or excluded points) and (v) "wetted" by the fluid within the grid on one and *only* one side.

   The resulting boundary segments are considered to belong to one of the J or K constant index classes and are numbered in any convenient manner, starting with 1, within each class. The example problem's boundaries are split into five segments with two in the J constant class and three in the K constant class and have been appropriately numbered.

2. Determine the indices of each segment — this is generally an automatic by-product of the first step.

3. Find the sign of the surface normal for each segment — this is determined by using the index increment required to move from the constant index surface of the segment to the similar constant index surface within the flow field. For example, consider the case of a segment in a K constant surface (bounded by the same J and L limits as the K constant segment) is within the flow field, then the unit normal is -1. If this procedure results in an ambiguous unit normal, then the segment has been incorrectly specified, if so the first step must be repeated with care.

TABLE A-1. BOUNDARY CONDITION TYPES

Code	Description	Auxiliary Variables
-10	Fixed conditions	None
0	Free boundary	Total, static pressure and total temperature
50	Slip surface	None
51	Axis of symmetry	None
60	No-slip wall, adiabatic	None
60	No-slip wall, isothermal	Wall temperature
91-96	Specified mass flux	Mass flux and total Temperature

4. Determine the desired boundary condition code and any auxiliary variables — each boundary condition allowed for in the PARC code has a boundary condition type code assigned to it as shown below. Some of these also require auxiliary information (e.g., static pressure) are shown in table A-1, where the descriptions mean:

(a) Fixed Conditions: All flowfield values are held fixed at their initial values provided by the restart file. Suggested use is for known supersonic inflow boundary segments only.

(b) Free Boundary: Any boundary segment through which the fluid flow can freely pass and is not a known supersonic inflow or a mass flux boundary is considered to be a free boundary. Imposition of the correct inflow or outflow, supersonic or subsonic boundary condition is taken care of automatically. However, this boundary condition works best if the boundary segment is perpendicular to the direction of flow. Also, the auxiliary condition is the total pressure for subsonic inflow and static pressure for subsonic outflow.

(c) Slip surface: All flow gradients normal to this boundary segment's surface are taken to be zero, along with the component of velocity normal to the surface. This boundary condition also serves as a symmetry plane boundary condition.

(d) Axis of symmetry: This is very similar in function to the slip surface boundary condition; this boundary specification is specialized for application to the axis of symmetry for simulations using the axisymmetric option of the PARC code.

(e) No-slip wall, adiabatic: All velocity components and the normal gradients of pressure and temperature are set to zero on boundary segments using this option. The grid lines should be normal to this wall for best results.

(f) No-slip wall, isothermal: Similar to the boundary condition discussed above except that the surface temperature is set to that provided through the temperature auxiliary variable.

(g) Specified mass flux: This boundary condition functions very similarly to the free boundary condition except that the pressure is determined indirectly through the specified mass flux auxiliary variable. The last digit of this code (1 to 6) is used to control the relaxation of the pressure towards the value, which will produce the desired mass flux with one giving the fastest and six the slowest relaxation. The mass flux specified through the auxiliary variable is to be positive for flow into the flow field and negative for flow out of the flow field.

b. NAMELIST BOUNDS parameters — Once the boundaries are split into segments and the appropriate boundary condition information is determined for each segment, as described above, this information is input to the PARC code through parameters in the NAMELIST BOUNDS. The basic philosophy behind the use of these parameters is very similar to that used in assembling the boundary condition information in that a set of parameter vectors corresponding to particular segments within each class. This will be made clearer through the description of these parameters and the following example:

1. NJSEG, NKSEG: This parameter gives the total number of boundary segments for each of the J and K coordinate classes.

2. JLINE, KLINE: Integer vectors that identify the J and K constant index of each of the corresponding boundary segments within each coordinate class.

3. JTYPE, KTYPE: Integer vectors whose elements contain the appropriate boundary condition type code for each boundary segment.

4. JSIGN, KSIGN: Integer vectors that associate the sign of the surface normal with the corresponding boundary segment of each of the J and K constant index class.

5. PRESSJ, PRESSK: Auxiliary vectors whose elements contain the nondimensional values of total pressure for predominantly subsonic flow, static pressure for anticipated subsonic outflow, or signed mass flux for specified mass flux boundary segments (type codes 0, 0 and 91 - 96, respectively).

6. TEMPJ, TEMPK: Auxiliary vectors that specify the nondimensional total temperature for free boundaries or the wall temperature for no-slip walls (type codes 0 and 61, respectively) for each boundary segment.

The following integer parameter vectors associate the appropriate coordinate indices with each boundary segment. This association is coded into the parameter vectors name so that the first letter calls out the J or K constant index class, the second letter identifies the coordinate index being specified, and the remaining letters indicate whether this is the minimum (LOW) or maximum (HIGH) value of this index for the boundary segment. For example, JKLOW(2) = 15 is interpreted to mean that the minimum value of the K index for the second boundary segment in the J constant segment class is 15. The complete set of parameter vectors for this purpose are JKLOW, JKHIGH, KJLOW, and KJHIGH.

2.3 OUTPUT.

The printed output consists of two parts, (1) a record of the run parameters used and (2) convergence statistics generated during as the run progresses.

Various error messages may also appear in this file, identified by five leading asterisks.

2.3.1 Namelist Parameters.

The first part of the printed output written to unit 6 is a listing of the values of the Namelist parameters that will be used during the current execution of the PARC code. They are printed in groups corresponding to the individual Namelists. These tabulated values are not simple echoes of the input values as they are not printed immediately after they are read in and in that they include default values.

NAMELIST BOUNDS

```
$BOUNDS
  NJSEG = 2,
  JLINE(1)=1,JKLOW(1)=1,JKHIGH(1)=7,JTYPE(1)=-10,
  JSIGN(1)=1,
  JLINE(2)=9,JKLOW(2)=2,JKHIGH(2)=6,JTYPE(2)=0,
  JSIGN(2)=-1, PRESSJ(2)=0.0047, TEMPJ(2)=1.0,
  NKSEG = 3,
 KLINE(1)=1,KJLOW(1)=2,KJHIGH(1)=2,KTYPE(1)=50,
 KSIGN(1)=1,
 KLINE(2)=1,KJLOW(2)=3,KJHIGH(2)=9,KTYPE(2)=61,
 KSIGN(2)=-1, TEMPK(2)=0.5,
 KLINE(3)=7,KJLOW(3)=2,KJHIGH(3)=9,KTYPE(3)=-10,
 KSIGN(3)=-1,
$END
```

2.3.2 Convergence History.

The next portion of the printed output contains information on the behavior of calculations performed. This consists of a line of output at the frequency selected by the parameter NSPRT. Each line includes the iteration number (COUNT), time step scaling factor (DT), L_2 residual, and the magnitude and location of the maximum percentage change in either density or pressure (MAX PERCENT VARIATION). In addition, if selected by the parameter IFXPRT, this line of output will include a measure of the global conservation of mass, momentum, and energy (the net FLUKes).

2.3.3 Error Messages.

A variety of program generated error messages can occur at any point in the printed output, most of them indicating that execution is being terminated. It is best to examine both the Namelist values portion of the listing and the very end of the printable output for error messages even if the run appeared to terminate normally. Most of the errors checked for will occur during run initiation, whereas those that happen in the course of execution will cause the program to attempt to terminate with a normal printout and a restart file.

2.3.4 Plottable Output.

If selected by the option IPLOT, two files are written out, the grid information is written out to a file on unit 31, and the flowfield information at those grid points is written out to unit 30. These two files are written in the format required by the graphics postprocessor PLOT3D, which can be used for visual analysis of the results obtained

2.3.5 Restart File.

This is always written unless an error occurs during run initiation. This is the final state of the flow variables after NMAX iterations, and is written out with the grid information to unit 4 (fort.4). A filter program called convert is then invoked which converts this file to the input format used by the HINCOF-I code.

2.3.6 Example.

The program restart.f used to generate the initial conditions for one of the cases considered by the HINCOF-I code is listed on pages A-16 and A-17. The NAMELIST parameter file supplied as fort.9 for the case on pages A-16 and A-17 looks as on page A-18.

restart.f.

```
      PROGRAM ICFILE
      PARAMETER(JD=121,KD=64, THETA = 0 )
      DIMENSION R(JD,KD),RU(JD,KD),RV(JD,KD),E(JD,KD)
      DIMENSION X(JD,KD),Y(JD,KD)
      PARAMETER (G=1.4, GM1=G-1.)
      READ(1)X,Y

C  FORM THE ARRAYS OF NON-DIMENSIONAL CONSERVATION VARIABLES
C  CONSISTENT WITH FREE-STREAM MACH NUMBER 0.3.
      PI = ACOS( -1.0 )
      FMACH=.3
      FACT=(1.+.2*FMACH**2)
      PBAR=FACT**(-3.5)/G
      RHOB=FACT**(-2.5)
      RHOU=RHOB*FMACH*SQRT(1./FACT)
      EBARIN=PBAR/GM1+.5*(RHOU**2)/RHOB
      EBAR=PBAR/GM1
      DO 4 K=1,KD
      DO 4 J=1,JD
      R (J,K)=RHOB
      RU(J,K)=0
      RV(J,K)=0
      E (J,K)=EBAR
4     CONTINUE
```

```
      DO 5 K=1,KD
      E(1,K)=EBARIN
      RU(1,K)=RHOU * COS( THETA * PI/ 180.0 )
      RV(1,K)=RHOU * SIN( THETA * PI/ 180.0 )

5     CONTINUE

      FMACH=.5
      FACT=(1.+.2*FMACH**2)
      PBAR=FACT**(-3.5)/G
      RHOB=FACT**(-2.5)
      RHOU=RHOB*FMACH*SQRT(1./FACT)
      EBARIN=PBAR/GM1+.5*(RHOU**2)/RHOB
      DO 6 K=1,32
      E(121,K)=EBARIN
      RU(121,K)=RHOU * COS( THETA * PI/ 180.0 )
      RV(121,K)=RHOU * SIN( THETA * PI/ 180.0 )
6     CONTINUE

C  WRITE RESTART TAPE
      NC1=0
      WRITE(2)NC1,G
      WRITE(2)JD,KD
      WRITE(2)X,Y
      WRITE(2)R,RU,RV,E
      REWIND 2
      END
```

Namelist parameter file

```
$INPUTS
  NMAX=1000,      NP=1000,
  PREF=15.0,      TREFR=600.,
  IFXPRT=1,       NBLOCK=1,
  DIS2=0.1,      DIS4=0.24,
  DTCAP= 0.5,      PCQMAX=5.0,
  NSPRT=50,       IAXISY=0,       STOPL2=1.E-20,
  IPLOT=0,        RE=1.5E06,
$END
$BLOCK
  NPSEG=0, INVISC(1)=1,INVISC(2)=1,
  LAMIN(1)=1,LAMIN(2)=1,
$END
$BOUNDS
  NJSEG=3,
    JLINE(1)=1,
    JKLOW(1)=1,  JKHIGH(1)=64,         JTYPE(1)=-10,
    JSIGN(1)=1,
  JLINE(2)=121,
    JKLOW(2)=1,  JKHIGH(2)=31,         JTYPE(2)=-10,
    JSIGN(2)=-1,
  JLINE(3)=121,
    JKLOW(3)=33,  JKHIGH(3)=64,          JTYPE(3)=0,
    JSIGN(3)=-1,  PRESSJ(3)=0.672815,  TEMPJ(3)=1.0,
NKSEG=6,
  KLINE(1)=1,
    KJLOW(1)=1,  KJHIGH(1)=90,         KTYPE(1)=50,
    KSIGN(1)=1,
  KLINE(2)=64,
    KJLOW(2)=1,  KJHIGH(2)=121,          KTYPE(2)=0,
    KSIGN(2)=-1, PRESSK(2)=0.67285,      TEMPK(2)=1.0,
  KLINE(3)=31,
    KJLOW(3)=50,  KJHIGH(3)=121,         KTYPE(3)=60,
    KSIGN(3)=-1,
  KLINE(4)=32,
    KJLOW(4)=50,  KJHIGH(4)=121,       KTYPE(4)=50,
    KSIGN(4)=1,
  KLINE(5)=1,
    KJLOW(5)=90,  KJHIGH(5)=121,         KTYPE(5)=60,
    KSIGN(5)=1,
$END
```

3. REFERENCES.

1. Albers, J.A., and Stockman, N.O., "Calculation Procedures for Potential and Viscous Flow Solutions for Engine Inlets," *Journal of Engineering for Power*, pp. 1-10, January 1975.

2. Stockman, N.O., and Farrell Jr., C.A., "Improved Computer Programs for Calculating Potential Flow in Propulsion System Inlets," NASA Technical Memorandum 73728, July 1977.

3. Cooper, B.K., The PARC Code: Theory and Usage, Arnold Engineering Development Center Report, AEDC-TR-87-24, October 1987.

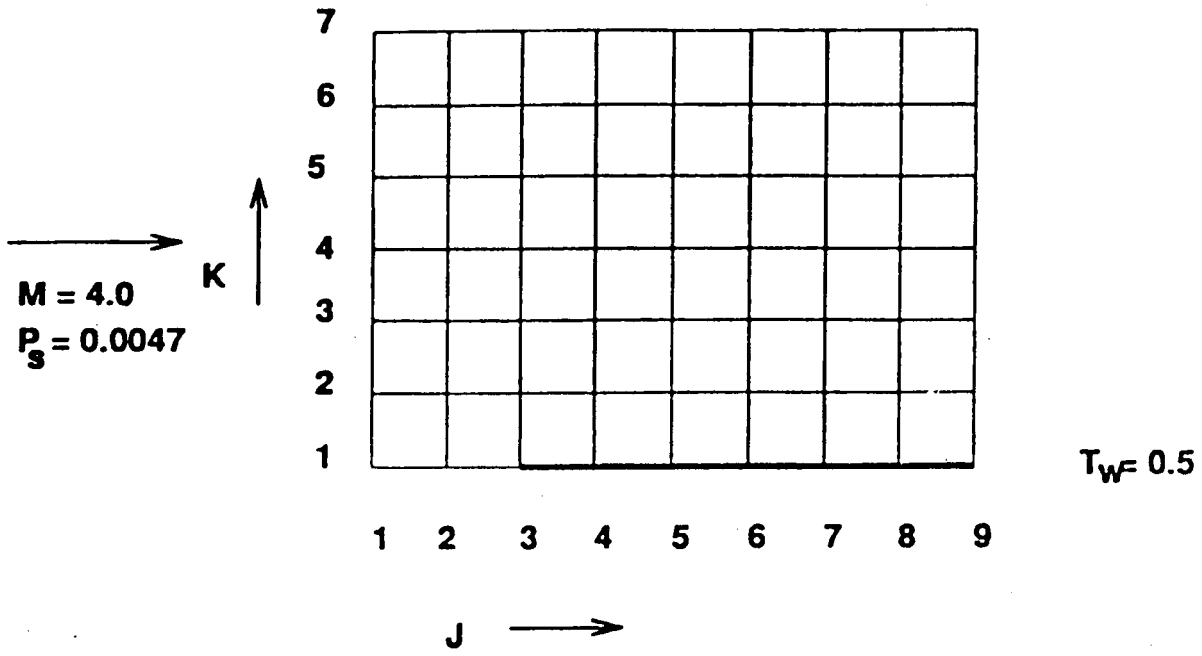

FIGURE A-1. EXAMPLE BOUNDARY SPECIFICATION PROBLEM

APPENDIX B
LISTING OF VARIABLES

Ao – Maximum contact area between hail and inlet surface
CH – Specific heat capacity of hail
CORE – The height of the core region at the engine face
Cd – Drag coefficient of hailstone
Dt – Time step for the Runge-Kutta method
Dwa – Diffusion coefficient of water in air
Eice – Youngs' modulus of hail
Esh – Saturation vapor pressure over hailstone
Esurface – Youngs' modulus of inlet material
Fnc – Fraction by number of hailstones entering core stream
Fne – Fraction by number of hailstones entering at engine face
Fvc – Fraction by Volume of hailstones entering at core stream
Fve – Fraction by Volume of hailstones entering at engine face
G – Constant of gravity
HAIL – Structure describing a hailstone and its associated properties
HAILTEMP – Energy hail temperature
KG – Thermal conductivity of air
LF – Latent heat of fusion of hail
MUF – Coefficient of kinetic friction between hail and inlet material
MUinf – Viscosity of air at freestream
Mass – Mass of hailstone
NB – Number of surfaces for the inlet
NX – Number of nodes in X direction for the air flowfield grid
NY – Number of nodes in Y direction for the air flowfield grid
Niter – Number of iterations per simulation
Np – Number of hailstones entering per batch
Omega – Angular velocity of hailstone
Po – Maximum impact force
Qcc – Heat transfer due to conduction and convection processes
Qesc – Heat transfer due to sublimation processes
R – Radius of hailstone
RH – Relative humidity
RHO – Density of air
RHOH – Density of hail
Re – Particle Reynolds number
Seed – Seed number for the random number generator
SizeF – Choice of pdf for the size of the hailstone
TNP – Maximum number of hailstones
Tair – Temperature of air
Temp – Temperature of hailstone
Tsim – Duration of each simulation

Vrel – Relative velocity between hailstone and air
Vxair – Velocity of air in X direction
Vxp – Velocity of hailstone in X direction
Vyair – Velocity of air in Y direction
Vyp – Velocity of hailstone in Y direction
X – X-value at a node for the air flowfield grid
Xp – Location of hailstone in X direction
Y – Y-value at a node for the air flowfield grid
Yp – Location of hailstone in Y direction
acc – Centrifugal acceleration imposed on the hailstone
active – Flag indicating hailstone is present in the flowfield grid
alpha – Angle of impact between two impacting hailstones
collision – Counter indicating number of interparticle collisions
core – Flag indicating entry into core stream
engine – Flag indicating entry into engine stream
f – Pointer to position of a hailstone
fd – Pointer to velocity of a hailstone
i – Number identifying a hailstone
impact – Flag indicating break-up on impact
introj – Interval between entry of fresh batches of hail
ix – X location of grid node closest to the hailstone
iy – Y location of grid node closest to the hailstone
j1 – Grid node index for an inlet surface or spinner
j2 – Grid node index for an inlet surface or spinner
k – Grid node index for an inlet surface or spinner
nactive – Number of hailstones that have entered the flowfield
nc – Number of hailstones entering core stream
ne – Number of hailstones entering at engine face
ni – Global iteration counter
ntotal – Number of hailstones introduced over a simulation
nup – Poisson's ratio for hail
nus – Poisson's ratio for inlet material
nx – Normal to an inlet surface, X-component
ny – Normal to an inlet surface, Y-component
omegas – Angular velocity of spinner
pdfchoice – Choice of velocity pdg
q – Radio of masses of two impacting hailstones
r – random number
rn – Normal coefficient of restitution
slope – Slope of the inlet surface or spinner at impact point
tcontact – Time of contact
troll – Time of roll
tslip – Time of slip
vc – Volume of hailstones entering core stream
ve – Volume of hailstones entering at engine face

vtotal – Volume of hailstones introduced over a simulation
wall – Counter indicating number of impacts with inlet surfaces

APPENDIX C
LISTING OF SUBROUTINES

Activate: This function serves to introduce new batches of particles, Np in number at a time, into the flowfield at certain fixed intervals of time given by the probability density function in figure 2. This function also assigns the location of appearance, the velocity and radius for the hailstones at entry based on the appropriate probability density functions. The velocity and the radius of the hailstones are assigned based on the choice of the probability density function, which is input from the main program. The function returns the number of hailstones that have been activated over the duration of the whole simulation.

i. Input Variables: nactive, Np, SizeF
ii. Output Variables: Vxp, Vyp, R
iii. Usage: int Activate(int nactive,int Np,double SizeF)

Advance: This function advances the hailstones through each time step. It passes the values of the location and the velocity of each hailstone to the Runge-Kutta function which advances the hailstones by a time step. The new position and the velocity of each hailstone are then stored for display.

i. Input Variables: Dt, ni
ii. Output Variables: Xp, Yp, Vxp, Vyp
iii. Usage: void Advance(double Dt,int ni)

Checkb: This function checks to see if any hailstone has impacted with any of the inlet surfaces or the spinner. It calculates the point of intersection of the trajectory of the hailstone with an inlet surface or the spinner. If the hailstone is in the vicinity of the intersection point, within a distance less than or equal to the radius of the hailstone, the hailstone is assumed to have impacted the inlet surface or the spinner, otherwise the function checks for the next active hailstone, where the word active denotes whether the hailstone is present in the computational grid. If the hailstone is found to impact any surface, then the function Impactw is called to handle the impact. The angle of incidence at impact is computed and passed to the function Impactw. Also, if the impact is with a spinner surface, the centrifugal acceleration imposed on the hailstone is computed and passed to Impactw.

i. Input Variables: k,j1,j2,i
ii. Output Variables: wall
iii. Usage: void checkB(int k,int j1,int j2, inti)

Checkw: This function enables each inlet surface and spinner surface to be checked. It calls the function Checkb for each surface.

i. Input Variables: None
ii. Output Variables: None

iii. Usage: void CheckW(void)

Checkp: This function checks for collisions between hailstones. It checks to see if the distance between any two hailstones is less than or equal to the sum of their radii. If true, the two are assumed to have impacted each other and the function Impactp is called to handle the processes associated with a collision. The angle of impact between the two impacting bodies is passed to this function along with the ratio of the masses of the two hailstones. The counter, collision, is incremented for each collision that each hailstone undergoes.

i. Input Variables: None
ii. Output Variables: collision
iii. Usage: void CheckP (void)

Conv: This function checks whether the convergence criterion CF, given in eq. (29), has been satisfied after each simulation. It computes the values of the four fractions, given in eqs. (25-26), and determines if the volume fraction is within a certain specified tolerance. If true, the simulation is terminated and the function Output is called to write out the final results.

i. Input Variables: nactive
ii. Output Variables: CF
iii. Usage: void conv(int nactive)

Fsub: This is the function called by the Runge-Kutta time stepping scheme for each hailstone, where the location and velocity of the hailstone are defined. The relative velocity between the air flowfield and the hailstone is computed and the particle Reynolds number is calculated. Based on this Reynolds number, the appropriate drag coefficient of each hailstone is computed. This value is then used in the expression for the momentum equation in Lagrangian form. The variables f and fd are pointers to the position and the velocity of the hailstone respectively.

i. Input Variables: i
ii. Output Variables: f,fd
iii. Usage: void fsub(int i,double *f,double *fd)

Gety: This function locates the hailstone with equal chances of appearing anywhere along the freestream station O, defined in figure 1. It locates all hailstones in a batch in such a fashion that no two hailstones are closer than a certain minimum distance, to prevent overlap of the hailstones.

i. Input Variables: nactive,Np
ii. Output Variables: Yp
iii. Usage: int Gety(int Np, int nactive)

Heat: This function calculates the heat transfer due to sublimation or melting processes wherever appropriate. This heat transfer may also lead to a change in the size of the hailstone, and

hence is important in influencing the trajectory of the hailstone. The temperature of the hailstone and the surrounding air, which are input to the function, determine the nature of the heat transfer processes it may undergo. The final radius and temperature of the hailstone are output.

i. Input Variables: Dt,RH
ii. Output Variables: R,Temp
iii. Usage: void Heat(double Dt, double RH)

Impactbnd: Each inlet surface or spinner boundary is shifted outward by the radius of a hailstone. This is done to determine the impact point of the hailstone accurately on any of the boundaries. This shifting is accomplished by moving each of the nodes on the boundary by an appropriate distance along the outward normal.

i. Input Variables: None
ii. Output Variables: nx,ny
iii. Usage: void impactbnd(void)

Impactp: This function handles the impact processes between any two hailstones. The equations of momentum along the tangential and normal direction to the line of impact are solved for together with the value for the normal coefficient of the restitution. Since the radii of curvature of the hailstones are so small, the time of contact between hailstones during impact are exceedingly small, and hence the tangential coefficient of restitution is taken to be 1. The result in the form of the final velocities after impact is passed back to the main program. Here, the variables i and j identify the impacting hailstones.

i. Input Variables: alpha, q, i,j
ii. Output Variables: V xp, V yp
iii. Usage: void ImpactP(double alpha,double q, int i, int j)

Impactw: This function handles the impact of a hailstone with any of the inlet surfaces or the spinner. The impact processes, including the computation of the time of slip and the time of roll, are handled in this function. The contact area, the contact force, the coefficient of sliding friction and the contact time together determine the tangential restitution. The angular momentum that is imparted to the hailstone as well as the angular velocity that may already be possessed by the hailstone is accounted for during this process. The centrifugal acceleration, if present, is applied to the rebounding hailstone over a fraction of the contact time. The final results in terms of the rebound normal and tangential velocities of the hailstone are passed back to the main program.

i. Input Variables: slope,i,acc
ii. Output Variables: V xp, V yp
iii. Usage: void ImpactW(double slope, int i,double acc)

Introduce: This function determines the time interval between entry of fresh batches of hailstones. This function returns the number of iterations towards the next call to the function Activate.

i. Input Variables: r,Dt
ii. Output Variables: introj
iii. Usage: int introduce(double r, double Dt)

Locatep: This function locates the hailstones in the computational grid for the air-flowfield, since the velocities for the air-flowfield are known only at the nodes on the computational grid. The air velocity at the position of the hailstone is needed to determine the particle Reynolds number, and the aerodynamic drag force on the hailstone. The flags, core, and, engine, are set appropriately if the hailstone enters the corresponding region at the engine face.

i. Input Variables: None
ii. Output Variables: ix,iy,core,engine
iii. Usage: void LocateP(void)

Main: This is the main program where the necessary input information is read in and the variables are initialized. The air-flowfield, which is computed by another program, is read from the file Input.dat, and the different functions are called in order for each process.

i. Input Variables: None
ii. Output Variables: None
iii. Usage: int main(void)

Runge: This function implements the Runge-Kutta time stepping scheme and invokes calls to the function Fsub where the equations of motion are defined.

i. Input Variables: i,f,Dt
ii. Output Variables: None
iii. Usage: void Runge(int i,double *f, double Dt)

Output: This writes the final output of the simulation to a file called Output.dat. The ingestion characteristics, given by the fractions Fne, Fnc, Fve, and Fne, are written to the file together with the flags core, engine, wall, and collision for each hailstone. Also, the trajectory of each hailstone is written to the file XY.dat.

i. Input Variables: nactive
ii. Output Variables: Fnc,Fvc,Fne,Fve,Xp,Yp,Vxp,Vyp,wall,collision,engine,core
iii. Usage: void Output(int nactive)

☆U.S. GOVERNMENT PRINTING OFFICE: 1995 - 604-081/20105

Technical Report Documentation Page

1. Report No.	2. Government Accession No.	3. Recipient's Catalog No.
DOT/FAA/CT-94/80		

4. Title and Subtitle	5. Report Date
HINCOF-I: A Code for Hail Ingestion in Engine Inlets	August 1995
	6. Performing Organization Code

7. Author(s)	8. Performing Organization Report No.
N. Gopalaswamy and S.N.B. Murthy	M/FAA/002-94-1

9. Performing Organization Name and Address	10. Work Unit No. (TRAIS)
Purdue Research Foundation Hovde Hall - Purdue University West Lafayette, IN 47907	
	11. Contract or Grant No. FAA 92-G-002

12. Sponsoring Agency Name and Address	13. Type of Report and Period Covered
Department of Transportation Federal Aviation Administration Technical Center Atlantic City International Airport, NJ 08405	Interim Report May 10, 1992 through February 1994
	14. Sponsoring Agency Code AAR-432

15. Supplementary Notes

FAA Technical Monitor: Joseph Wilson

16. Abstract

One of the major concerns during hail ingestion into an engine, when an aircraft flies through a hail storm, is the resulting amount and space- and time-wise distribution of hail at the engine face for a given geometry of inlet and set of atmospheric and flight conditions. The appearance of hail in the capture streamtube is invariably random in space and time, with respect to size and momentum. During the motion of a hailstone through an inlet, a hailstone undergoes several processes, namely impact with other hailstones and material surfaces of the inlet and spinner, rolling and rebound following impact, heat and mass transfer, phase change, and shattering, the latter three due to friction and impact. Taking all of these factors into account, a numerical code, designated HINCOF-I, has been developed for determining the motion of hailstones from the atmosphere, through an inlet, up to the engine face. The numerical procedure is based on the Monte-Carlo method. The report presents a description and details of the code, along with several illustrative cases. The code can be utilized, in particular, to relate the spinner geometry — conical or, more effectively, elliptical — to the possible diversion of hail at the engine face into the bypass stream. The code is also useful for assessing the influence of various hail characteristics on the ingestion and distribution of hailstones over the engine face.

17. Key Words	18. Distribution Statement
Water Ingestion, Hail Ingestion, Turbo Fan	This document is available to the public through the National Technical Information Service (NITS), Springfield, Virginia 22161.

19. Security Classif. (of this report)	20. Security Classif. (of this page)	21. No. of Pages	22. Price
Unclassified	Unclassified	72	